Ana Rita Abrantes Dias

THE ROLE OF SIRTUIN 2 IN OLIGODENDROGLIA ON DOPAMINERGIC NEURON DIFFERENTIATION AND REGENERATION

Master Thesis in Biomedical Research

June / 2016

· U C ·

UNIVERSIDADE DE COIMBRA

Supervisor: **Prof. Dr. Tiago Outeiro**, Director of the Dept. Neurodegeneration and Restorative Research, University Medical Center Göttingen, Germany

Co-supervisor: **Dra. Éva Szegő**, Dept. of Neurodegeneration and Restorative Research, DFG Research Center for Nanoscale Microscopy and Molecular Physiology of the Brain University Medical Center Göttingen, Germany

Internal supervisor: **Dr. Henrique Girão**, Director of the Dept. Protein Quality Control in Health and Disease, Faculdade de Medicina da Universidade de Coimbra, Portugal

ACKNOWLEDGEMENTS

I would like to start by thanking Prof. Dr. Tiago Outeiro, for allowing me this great opportunity to work in such a prestigious lab. The things I've learned there, I will carry them through all my life.

Especially to Dr. Éva Szegő, my patient and caring direct supervisor, I owe everything that I learned throughout this year. Your passion for your work is my inspiration. Thank you so much for all the sweat you put into making me a better scientist.

To the soon-to-be great Dr. Raquel Pinho, my motivator, I'll always be grateful for your advices and infinite serenity. To Dr. Ellen Gerhardt, thank you so much for your help with the plasmid preparations and for being my companion on the latest working hours. To Christiane Fahlbusch, thank you for your tireless help with preparing the virus, and for being our priceless number one sidekick.

To Dr. Laetitia Francelle, all your advice was precious to me. You never ever fail to lend a hand. I'm so happy to call you a friend! And to Dr. Vaishali Sharma, your kind spirit makes me smile, every day. I'm so happy I met you!

To Kristine Hutalle, her work in the background kept this lab moving forward. To Diana Lázaro, from whom the pettiest questions were always addressed in the most helpful way. To Dr. Maria Pavlou, whose curious spirit instigate us all to progress.

To Sonja Reisenauer, our connector to the German world; to Omar Díaz, the smiley man of a million languages; and to Daniela Proto, with the most contagious energy and happiness, your help behind the desk is incredibly fundamental and most appreciated!

To Dr. Tomás Lopes da Fonseca, Dr. Anna Villar-Piqué, Marina Marques, Sindhu Thiagarajan, Nicole Weigelt, and to all the people that crossed our lab during this year, it was a big, big pleasure.

Finally, the hugest thank you to the most amazing companions in this town. Mariana Dias, Belisa Russo, Isabel Paiva, Rayne Magalhães, and Dr. Aline Brasil. Whether by sharing a conversation while having a beer, whether by sharing nights at the lab and a million scientific questions - I hope you know that I could not have survived without you by my side, at all times.

Back home, I owe a couple of "thank yous" as well:

To Clara Pereira and Prof. Vasco Barreto, to João Pinto Ferreira and Prof. Alexandrina Mendes, and to Dr. Pedro Gomes and Prof. Cláudia Cavadas. You were the ones who taught me all my foundations and gave me the confidence to become more than just a prototype of a scientist.

To all my friends, who have this wonderful tendency to believe more in me, than I do in myself. I cannot address you all individually, as words would never be enough – especially to you, Ana Leal. To all of you who battle life by my side. Just remember that "countries are just lines drawn in the sand" – to all of us

around this world, physical distance is not capable to keep us apart. My ladies from Santarém, my buddies from Lisboa, my MIBs from Coimbra, my Erasmi from Pavia. And now, my gang from Göttingen.

At last, but never the least, my biggest appreciation of all goes to my whole family. I often wonder how you can make all of this possible, and I truly hope to someday repay all your trust and care. To my mom, my dad, my baby brother… thank you. I am your biggest fan. We are one.

TABLE OF CONTENTS

INDEX OF FIGURES

INDEX OF TABLES

LIST OF ABBREVIATIONS

µg	Microgram
µL	Microliter
µM	Micromolar
°C	Degrees Celsius
A	Ampère
AD	Alzheimer's disease
APS	Ammonium persulfate
ATP	Adenosine triphosphate
BSA	Bovine Serum Albumin
CMF	Calcium & Magnesium free
CNP	2',3'-Cyclic-nucleotide 3'-phosphodiesterase
CNS	Central nervous system
CR	Calorie restriction
DA	Dopamine
DAB	3,3'-diaminobenzidine
ddH_2O	Bi-distilled water
DMEM	Dulbecco's modified Eagle's medium
DMSO	Dimethyl sulfoxide
DNA	Deoxyribonucleic acid
ECAR	Extracellular acidification rate
ECL	Enhanced Chemiluminescence
EGFP	Enhanced green fluorescent protein
FBS	Fetal Bovine Serum
FCCP	Carbonyl cyanide-4-(trifluoromethoxy)phenylhydrazone
g	G-force or RCF (relative centrifugal force)
GFP	Green fluorescent protein
HBSS	Hank's balanced salt solution
HDACs	Histone deacetylases
ICC	Immunocytochemistry
IHC	Immunohistochemistry
kDa	kilo Dalton
KO	knockout
LBs	Lewy bodies
LB medium	Luria-Bertani medium

LV	Lentivirus
M	Molar
MAG	Myelin-associated glycoprotein
MBP	Myelin basic protein
MEM	Minimum Essential Medium Eagle
mL	Mililiter
mM	Millimolar
MPP+	1-methyl-4-phenyl pyridinium
MPTP	1-methyl-4-phenyl-1,2,3,6-tetrahydropyridine
NaCl	Sodium chloride
NAD+	Nicotinamide adenine dinucleotide
OCR	Oxygen consumption rate
OMgp	Oligodendrocyte/myelin glycoprotein
ON	Overnight
P/S	Penicillin-streptomycin antibiotics
PBS	Phosphate buffered saline
PD	Parkinson's disease
PFA	Paraformaldehyde
PLL	Poly-L-lysine
PLO	Poly-L-ornithine
PNS	Peripheral nervous system
RT	Room temperature
Sir2	Silent information regulator protein 2
SIRT	Silent information regulator-like protein
SDS-PAGE	Sodium dodecyl sulfate Polyacrylamide gel electrophoresis
SNpc	Substantia nigra pars compacta
TBS	Tris buffered saline
TBS-T	Tris buffered saline + Tween
TE	Tris EDTA buffer
TEMED	Tetramethylethylendiamin
TH	Tyrosine hydroxylase
V	Volt
WB	Western Blot
WT	Wild-type

ABSTRACT

Parkinson's disease (PD) is a neurodegenerative disorder, characterized by an extensive dopaminergic neuron loss from the substantia nigra pars compacta (SNpc), resulting in synaptic loss in the striatum and in reduced dopamine levels. The ability to regenerate of the still existing neurons is very low or inhibited. Sirtuins are a family of proteins highly expressed in the central nervous system (CNS). The NAD+-dependent deacetylase Sirtuin 2 (SIRT2) is present in many CNS cells, and was described to be expressed by oligodendrocytes and modulate oligodendroglial differentiation possibly through its tubulin deacetylation activity. Therefore, we hypothesized that SIRT2 might influence the differentiation of dopaminergic neurons and axonal regeneration by modulating a) oligodendroglial and b) neuronal functions.

In the present study, we attempted to elucidate the role that SIRT2 plays in oligodendrocytes and how relevant this could be for the development of the SNpc and for neuronal regeneration. We addressed these questions by analyzing the number of tyrosine-hydroxylase-positive (TH+) dopaminergic neurons in the SNpc of conditional neuronal and oligodendroglial Sirt2-KO mice, and further explored the role of oligodendroglial SIRT2 in two distinct cell models.

We observed that SIRT2 overexpression exerts potentially beneficial effects on cell metabolism in OLN-93 oligodendroglial cells. Since the ratio of oligodendroglia in primary cortical cultures is low, we could not detect changes in the levels of ubiquitously expressed or neuronal proteins, such as GAP-43. Interestingly, although the oligodendroglial CNP expression was not altered, differentiation of those cells might change. Along with the absence of GAP-43 regulation, we also did not detect changes in axonal regeneration in the scratch model. However, when SIRT2 is missing during the total development of the brain, it affects the number of TH+ cells in the SNpc, as we found less dopaminergic neurons in the SNpc of neuronal Sirt2-KO mice, and more in oligodendroglial Sirt2-KO mice.

In summary, oligodendroglial SIRT2 plays an important role in neuronal development in the SNpc, most probably in terminating the differentiation progress. In contrast, neuronal SIRT2 seems to be important for the differentiation per se. Additionally, oligodendroglial SIRT2 regulates mitochondrial respiration.

Our study contributes to the understanding of the SIRT2-mediated axonal-glia interaction, in particular in dopaminergic neuronal differentiation. This may impact on the molecular mechanisms underlying PD, and may open novel avenues for the development of effective therapeutic strategies against this devastating disorder.

1. INTRODUCTION

1.1. Parkinson's disease (PD)

The frequency and prevalence of neurodegenerative disorders has been growing worldwide, due to the increase in life expectancy and the aging of overall populations (World Health Organization, 2006).

Parkinson's disease (PD) affects more than seven million people in the world, being the second most common neurodegenerative illness, after Alzheimer's disease (Schlossmacher, 2007). Age is the major risk factor for the development of this disorder, as meta-analysis showed a steady increase in PD prevalence with age across all regions of the world (Pringsheim et al., 2014).

PD was first described in "An essay on the shaking palsy" (Parkinson, 1817). PD patients present essentially four distinct clinical motor features: tremor at rest, rigidity, bradykinesia and postural instability (Gelb et al., 1999; Jankovic, 2008) .The majority of cases present also several variable non-motor symptoms such as fatigue, depression, anxiety, impaired sense of smell, constipation, sleep disorders and cognitive and behavioral problems (Jankovic, 2008; Pandya et al., 2008).

Pathologically, PD is characterized by the accumulation of Lewy Bodies (LB) in the surviving neurons. LB are spherical eosinophilic cytoplasmic protein aggregates found in all affected brain regions, consisting primarily of α-synuclein, but also of synphilin-1, parkin and ubiquitin, among numerous other proteins (Kuzuhara et al., 1988; Schlossmacher et al., 2002; Spillantini et al., 1998; Wakabayashi et al., 2000, 2007).

Still, the main hallmark of PD is the loss of dopaminergic neurons in the nigrostriatal pathway (Gelb et al., 1999; and review by Dauer and Przedborski, 2003). The nigrostriatal pathway is one of the four major dopamine pathways in the brain, neural trails responsible for conducting the neurotransmitter dopamine in-between brain regions. This pathway is particularly involved in the production of movement. It is composed of dopaminergic neurons whose cell bodies are located in the midbrain's substantia nigra pars compacta (SNpc), projecting to the basal ganglia and synapse in the striatum, located in the forebrain. The degeneration of these neurons in PD, which normally contain noticeable amounts of neuromelanin (Fedorow et al., 2005), produces classic SNpc depigmentation and depletion of dopamine (DA) (**Fig. 1.1-1**). When symptoms start to be noticed, around 60% of SNpc dopaminergic neurons have already been lost and around 80% of striatum putamenal DA is depleted (Bernheimer et al., 1973).

Tyrosine Hydroxylase (TH) is the rate-limiting enzyme of catecholamine synthesis, from which dopamine takes part. Hence, it is considered one of the major molecular agents in determining dopamine levels in the brain (review by Daubner et al., 2011). The degree of loss of striatal DA and TH activity appears

to be more prominent than the loss of nigral DA and TH activity or cell bodies. For this reason, it was proposed that in PD, neurodegeneration may be a "dying-back" process that begins in the striatal terminals (Hornykiewicz, 1998). Interestingly, the mesolimbic dopaminergic system originating in the ventral tegmental area (VTA) is much less affected in PD (Uhl et al., 1985).

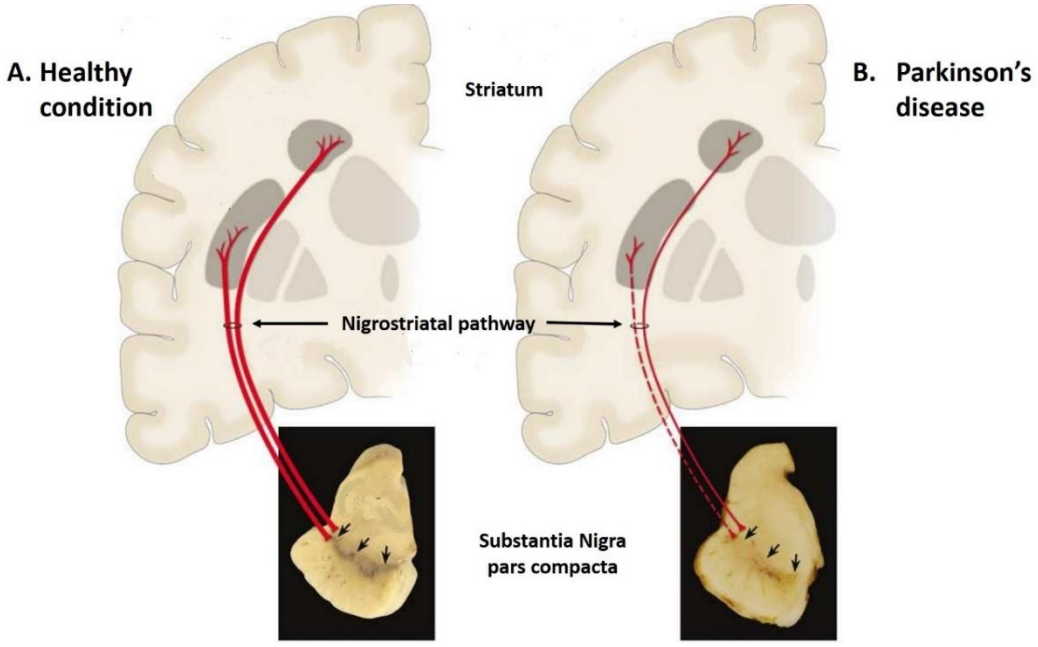

Figure 1.1-1. Schematic depiction of the nigrostriatal pathway. (A) Healthy brains present a normal nigrostriatal pathway (in red) composed of dopaminergic neurons whose cell bodies are located in the SNpc, and whose axons project to the striatum. The SNpc has a dark pigmentation due to the production of neuromelanin by DA neurons. **(B)** In PD, the nigrostriatal pathway is compromised, displaying evident depigmentation in the SNpc due to loss of dopaminergic neurons (adapted from Dauer and Przedborski, 2003).

1.1.1. Etiology of PD

Due to its very complex etiology, it is hard to define the precise events that trigger degeneration in PD. Even though age is an important risk factor for PD, the processes that produce age-related dopaminergic neuronal death seem to be different from those that occur in PD (Dauer and Przedborski, 2003). Nowadays, a "multi-hit" hypothesis is in order: genetic and environmental factors are both taken into consideration as the responsible for the development of this pathology, since they can promote protein misfolding, impairment of the ubiquitin-proteasome pathway, mitochondria dysfunction and oxidative stress (Sulzer, 2007). In order to achieve some distinctness, PD can be divided in sporadic or familial PD.

1.1.1.1. Familial PD

Although familial PD only accounts for little more than 10% of cases, there are numerous genes suggested to cause it. Familial cases of PD are categorized into autosomal-dominant and autosomal-recessive parkinsonism, depending on the causing gene (Sulzer, 2007; Coppedè et al., 2012). These seem to express proteins that fall into very distinct categories: proteins that distress mitochondria (e.g. PINK1, DJ-1, OMI/HTRA2 and POLG); proteins involved in organelle trafficking and vesicular fusion (e.g. a-syn and tau); proteins linked to macromolecular degradation pathways, such as ubiquitination or ubiquitination-like (e.g. parkin and DJ-1) and lysosomal function (e.g. b-glucocerebrosidase); proteins affecting oxidative stress or antioxidant function (e.g. sepiapterin, DJ-1 and fibroblast growth factor-20 (FGF-20)).

1.1.1.2. Sporadic PD

Sporadic PD accounts for almost 90% of all cases and, although the exact cause is still unclear, it is thought to arise due to environmental factors (Bellou et al., 2016), polygenic inheritance and complex gene-environment interactions (Coppedè et al., 2012).

Interestingly, several polymorphisms were identified as genetic risk factors for the sporadic form of PD, like polymorphisms in SNCA, Leucine-Rich Repeat Kinase 2 (LRRK2) and tau genes (Hardy, 2010).

Abnormalities in mitochondrial functions have also been linked to the development of neurodegenerative diseases, in particular of PD (reviews by Orth and Schapira, 2002; and by Keane et al., 2011). Brain cells are highly dependent on the oxidative metabolism of glucose, for which an intact oxidative phosphorylation machinery in mitochondria is essential. This machinery involves the respiratory complexes located at the inner membrane of the mitochondrion: complex I (NADH ubiquinone oxidoreductase), complex II (succinate ubiquinone oxidoreductase), complex III (ubiquinone–cytochrome c oxidase), complex IV (cytochrome c oxidase) and complex V (mostly called ATP synthase), plus ubiquinone and cytochrome c present in the inner membrane and the intramembrane space, respectively (review by DiMauro and Schon, 2003).

Sporadic PD patients have a deficiency in mitochondrial complex-I in the nigrostriatal pathway (Schapira, 1998). This type of research into mitochondrial involvement in the pathogenesis of PD began in 1983, with reports on Parkinson's-like symptoms among young drug users, which led to the identification of 1-methyl-4-phenyl-1,2,3,6-tetrahydropyridine (MPTP) as a byproduct of desmethylprodine, an opioid analgesic used for recreational purposes (Langston et al., 1983; review in 1984). Though not toxic itself, the lipophilic drug crosses the blood brain barrier where it is oxidized by mono-amine oxidase B (MAO B) of glial cells to N-methyl-4-phenylpyridinium (MPP+), the active form of the neurotoxin. MPP+ is then taken

up by dopamine transporters (DAT) of dopaminergic neurons, where it accumulates within the mitochondrial inner membranes. While in the mitochondria, MPP+ was posteriorly discovered to inhibit complex-I, where it interrupts the electron transport and release reactive oxygen species (ROS), leading to the depletion of ATP (Mizuno et al., 1987). Furthermore, inhibition of the mitochondrial complex-I results in the opening of mitochondrial permeability transition pores, permitting the release of cytochrome c, which will trigger pathways that will eventually culminate in apoptotic cell death (review by Nagatsu and Sawada, 2006).

Similarly to MPTP, rotenone is also a commonly used toxin in PD research (Greenamyre et al., 2003). This natural lipophilic compound, primarily used as an insecticide, is able to effortlessly cross the blood brain barrier and enter neuronal cells and intracellular organelles, such as mitochondria, without the need of transporters. Rotenone is a specific mitochondrial complex-I inhibitor, leading to the release of free radicals into the mitochondrial matrix and ROS formation, which induces toxicity along with behavioral and motor symptoms of PD in tested animals (Alam and Schmidt, 2002).

The oxidative stress imposed by these toxins is also thought to spawn an inflammatory state (Nagatsu and Sawada, 2006). Chronic administration of either toxins leads to the accumulation of LB-like fibrillary inclusions containing aggregated α-synuclein and ubiquitin in brains of both rodents and primates (Betarbet et al., 2000; Kowall et al., 2000; Lee et al., 2002), although this phenotype doesn't seem to be apparent in acute toxicity. In vitro immortalized and primary cell culture models were shown to exhibit the same manifestation (Kalivendi et al., 2004; Borland et al., 2008). Hence, both compounds are widely used nowadays in animal and cell-based PD research (Przedborski et al., 2001; Sherer et al., 2003; and review by Keane et al., 2011).

1.2. Sirtuins

1.2.1. Yeast Sir2

Studies of aging in *Saccharomyces cerevisiae* led to the discovery of a conserved family of four proteins (Ivy et al., 1985, 1986) involved in the regulation of mating type loci genes in yeast.

A member of this family, Silent information regulator 2 (Sir2), is the only one among the four capable of suppress the formation of toxic ribosomal DNA circles (Sinclair and Guarente, 1997) and takes part in the mechanism that silences genes near telomeres (Aparicio et al., 1991). Due to this fact, it was later found to extend lifespan by 50% of yeast with extra copies of the SIR2 gene, while SIR2 deletion reduced longevity (Kaeberlein et al., 1999).

SIR2-like proteins are now identified in almost all phyla, including prokaryotes and referred to as **Sirtuins** (Frye, 2000; and reviews by North and Verdin, 2004; and by Haigis and Sinclair, 2010).

1.2.2. Mammalian Sirtuins

Sirtuins belong to a class of histone deacetylases (HDACs). Despite their name, these classes of proteins act on both histone and non-histone substrates.

HDACs are grouped into three classes based on their homology to yeast transcriptional repressors: classes I and II share significant similarity to each other in their catalytic cores, and sirtuins fit in class III. The uniqueness of this class resides in sirtuins' catalytic domain, which requires nicotine adenine dinucleotide (NAD) as a cofactor (Finnin et al., 2001). In the presence of NAD+, sirtuins catalyze the deacetylation of an acetylated substrate, with O-acetyl-ADP-ribose and nicotinamide as side products (Schemies et al., 2010).

In humans, seven sirtuin orthologues have been identified (SIRT 1-7) which act primarily as lysine deacetylases, therefore modulating the activity of numerous substrates (Denu, 2005; and review by North and Verdin, 2004; and by Michan and Sinclair, 2007). Sirtuins are present in different type of tissues, such as liver, kidney, adipose tissue, skeletal muscle and in several areas of the brain.

Despite sharing their highly conserved catalytic domain, mammalian sirtuins are found in various of subcellular compartments (**Fig. 1.2-1**), and also differ in other aspects such as their flanking N- and C-terminals, in the variety of substrates that they utilize and in their protein binding partners (**Table 1.2-1**) (reviews by Guarente, 2011; and by Bheda et al., 2016) .

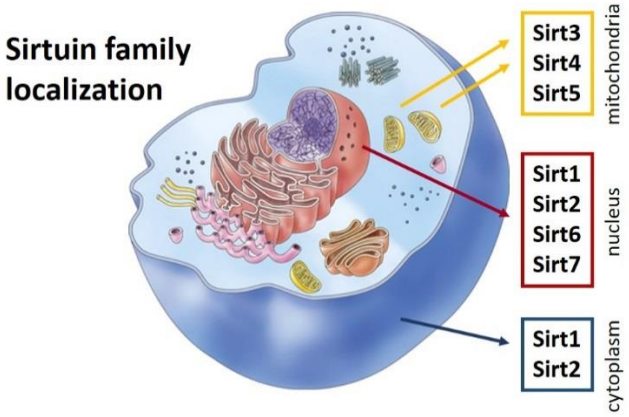

Figure 1.2-1. Subcellular distribution of sirtuin proteins. SIRT3-5 are localized in the mitochondria, while SIRT6 is nuclear and SIRT7 mainly nucleolar. SIRT1 and 2 are known to transiently shift between cytosol and nucleus.

Sirtuin	*MW (kDA)*	*Localization*	*Enzymatic activity*	*Interactors*
SIRT1	81.7	Nuclear, cytoplasmic	Deacetylase	Euchromatin p53, Ku70, PPARγ, PGC- 1α,NFκB, FOXO
SIRT2	43.2	Cytoplasmic, nuclear	Deacetylase	α-tubulin Histone H4
SIRT3	43.6	Mitochondrial	Deacetylase	Mitochondrial proteins AceCS2
SIRT4	35.2	Mitochondrial	ADP-ribosyltransferase	Glutamate dehydrogenase
SIRT5	33.9	Mitochondrial	Deacetylase, demalonylase, desuccinylase	unknown
SIRT6	39.1	Nuclear	ADP-ribosyltransferase, deacetylase	Heterochromatin DNA polymerase-β
SIRT7	44.8	Nucleolar	Deacetylase	Ribosomal DNA RNA polymerase-I

Table 1.2-1. Description of sub-cellular localization, activity and the main interactors of the human family of sirtuins. Molecular weight (MW). (adapted from Outeiro et al., 2008; Donmez and Outeiro, 2013; and Park et al., 2013.

SIRT1, 6 and 7 are nuclear sirtuins and have a role in transcriptional regulation, through targeting of transcription factors, cofactors or histones. SIRT 3, 4 and 5 are mitochondrial sirtuins and regulate enzymes activity and oxidative stress pathways. SIRT2 is the only sirtuin who resides mainly in the cytoplasm (Haigis and Sinclair, 2010; Donmez and Outeiro, 2013).

1.2.3. Sirtuins in neurodegeneration and in PD

Due to their correlation with aging, it is not surprising that sirtuins have been considered attractive research targets for understanding neurodegeneration, especially since this family of proteins was shown to be highly expressed in the central nervous system (CNS) (review by Duan, 2013).

SIRT1 is the most studied human sirtuin in neurodegenerative models, and these studies point to a potentially neuroprotective role of this sirtuin (review by Donmez and Outeiro, 2013). Regarding PD, the levels of SIRT1 in dopaminergic neurons are sharply decreased when treated with neurotoxins such as rotenone and MPTP (Pallàs et al., 2008), meaning that its levels might be reduced in PD patients. Calorie restriction (CR) was earlier reported to boost the levels of this protein in the brain, and studies have demonstrated that CR can protect against nigrostriatal damage in MPTP primate models of PD, thus suggesting that SIRT1 can prompt beneficial effects (Maswood et al., 2004). Additionally, pharmacological activation of SIRT1 by resveratrol, a naturally occurring polyphenol, was shown to protect against oxidative stress and α-synuclein toxicity in cellular models of PD (Albani et al., 2009). Furthermore, the

overexpression of SIRT1 in animal and cell models of PD was shown to combat the formation of α-synuclein aggregates (Donmez et al., 2012).

Mitochondrial SIRT3, 4 and 5 also seem to have important roles in mediating the CR-induced metabolic shift toward acetate and amino acid usage (Qiu et al., 2010). Postmortem studies on brains from aged-individual confirm also a correlation between a low-expressing gene polymorphism in SIRT5, and age-related decline in gene expression of PINK1 and DJ1/PARK7, genes crucial for mitochondrial function and related to familial PD cases (Glorioso et al., 2011).

1.2.4. SIRT2: an emerging target in PD

SIRT2 is localized along the microtubule network and shows striking preference for acetylated tubulin peptide as a substrate relative to acetylated histone H3 peptide. These observations establish SIRT2 as a preferential tubulin deacetylase (North et al., 2003).

Several transcript variants resulted from alternative splicing of this gene. Currently, there are four different human splice variants deposited in the GenBank sequence database. Yet, only transcript variants 1 (43.2 KDa) and 2 (39.5 KDa) have confirmed protein products of physiological relevance (Maxwell et al., 2011). It is said that, although SIRT2 localization is predominantly cytoplasmic, it transiently shifts between cytoplasm and the nucleus in a cell cycle-dependent manner (Vaquero, 2006). However, it was recently reported a 5th isoform (35.6 KDa) that appears to have a constitutive nuclear localization, even though it fails to show deacetylation activity (Rack et al., 2014).

SIRT2 is therefore associated with important roles in metabolic homeostasis (Gomes et al., 2015), cell cycle regulation (Inoue et al., 2007; Vaquero, 2006), tumor suppression (Kim et al., 2011), and in neurodegenerative diseases (Donmez and Outeiro, 2013).

SIRT2 was first linked to neurodegeneration when it was found that genetic or pharmacological inhibition of this protein was protective in models of PD (Outeiro et al., 2007). In this study, SIRT2 inhibition was correlated with rescue against α-synuclein toxicity in models of synuclein aggregation. In these models, SIRT2 inhibition resulted in fewer but larger aggregates of synuclein. It was thereby hypothesized that microtubule deacetylation by SIRT2, which accumulates with aging, might play an important role in α-synuclein aggregation. SIRT2 most probably affects microtubule transport-mediated aggresome formation by interfering with normal autophagy mechanisms in neuronal cells (Gal et al., 2012).

These findings also came in concordance to the most current view of synuclein aggregation, that larger fibrillary aggregates may be protective, in contrast to small but very toxic oligomers (review by Verma et al., 2015). This was later tested in other models of PD, including rat models overexpressing

mutated forms of α-synuclein (for review see Donmez and Outeiro, 2013); and also in regard to toxic aggregates of mutant huntingtin protein, related to Huntington's disease (Luthi-Carter et al., 2010). In both cases, it was confirmed the protective role of SIRT2 inhibition.

More recent studies from our group (unpublished) and others (Liu et al., 2014) have clearly shown that SIRT2 boosts nigrostriatal damage induced by MPTP. Congruently, they also demonstrated that this neurodegeneration could be prevented by genetic deletion of SIRT2 in MPTP-based mouse models of parkinsonism, without affecting brain development and morphology. The authors claim that this effect is achieved by SIRT2 due to the deacetylation of Foxo3a, that in turn activates a protein of the BCL-2 family called BIM, a well-known responsible for inducing cellular apoptosis (review by Brunelle and Letai, 2009).

1.3. The microenvironment of the brain: the glia

Glial cells constitute the large majority of cells in the nervous system (Sherwood et al., 2006). Despite their number and their role during development, their active participation in the physiology of the brain and the consequences of their dysfunction on the pathology of the nervous system have only been emphasized in the recent years. There are three types of glial cells in the mature central nervous system (**Figure 1.3-1**):

- **Astrocytes**, have elaborate local processes that give these cells a star-like appearance. These are the most numerous and diverse neuroglial cells in the CNS, and their major function is to maintain an appropriate chemical environment for neuronal signaling. Most of them express glial fibrillary acidic protein (GFAP) (review by Sofroniew and Vinters, 2010).
- **Microglia**, which share many properties with tissue macrophages, act primarily as scavengers that remove cellular debris. Following brain damage, the number of microglia at the site of injury increases dramatically. Some of these cells proliferate from microglia resident in the brain, while others come from macrophages that migrate to the injured area from the circulation (reviews by Lucin and Wyss-Coray, 2009; and by Saijo and Glass, 2011).
- **Oligodendrocytes** (or oligodendroglia), are responsible for generating myelin in the brain. Myelin is a highly specialized membrane structure enwrapping axons of the nervous system in successive concentric layers and has important effects on the speed of action potential conduction. In the peripheral nervous system (PNS), the cells that elaborate myelin are called Schwann cells (review by Bradl and Lassmann, 2010).

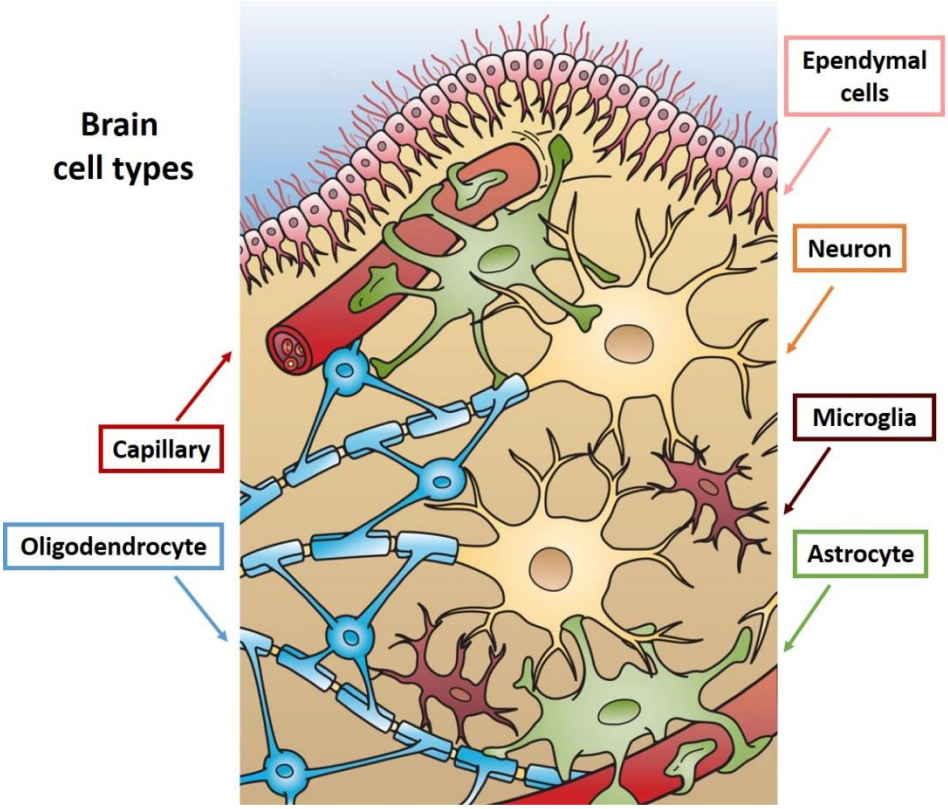

Figure 1.3-1. Illustration of the different cell types present in the brain. Neurons, glia cells (astrocyte, microglia and oligodendrocyte) and ependymal cells exemplified in fictitious colors. (adapted from Open Michigan Lectures)

1.3.1. Oligodendroglia and axonal regeneration

When the axons of a neuron are wounded, nerve function is restored by renewing the injured axons. GAP-43 is a specific phosphoprotein of neuron's presynaptic membrane, and is known to play a role in axonal outgrowth during development and nerve regeneration (Benowitz and Routtenberg, 1997). In fact, suppressing GAP-43 expression reduces growth cone formation, and overexpressing it induces spontaneous formation of aberrant connections (Aigner and Caroni, 1993; Aigner et al., 1995).

The SNpc is one of the many regions in the brain that seem to highly express this protein (Bendotti et al., 1991), which could lead to the conclusion that axons of DA neurons would be forced to regenerate upon lesion.

However, when it comes to PD, the ability of the remaining neurons in the SNpc to regenerate is very low or inhibited. This suggests that some inhibitory activity in the lesion site may be in place as a prevention mechanism for axon regeneration (Abe and Cavalli, 2008). Therefore, it has been explored the idea that both myelin formation and axonal growth ought to be tightly coordinated by axonal-glial interactions (Nave and Trapp, 2008).

The myelin membrane produced by oligodendrocytes insulates the axons and eases the rapid conduction of action potentials along the fibers. It is enriched in lipids and contains some unique proteins, such as the myelin basic protein (MBP) and proteolipid protein (PLP), among other not-so-specific proteins but still highly enriched in CNS myelin, such as 2',3'-Cyclic-nucleotide 3'-phosphodiesterase (CNP) and several glycoproteins. Each myelin segment alternates with the so-called "Nodes of Ranvier", intercalating unmyelinated sections of the axons which vary in length according to their location in the CNS, and at which sodium voltage-gated ion channels cluster. On the same axon, adjacent myelin segments belong to different oligodendrocytes (Morell and Quarles, 1999).

The formation of myelin is a highly regulated process, with different areas of the CNS having different degrees of myelination, as well as different classes of nerve fibers showing distinct patterns of myelination (review by Baumann and Pham-Dinh, 2001). Thus, a primary perturbation of myelinating glial cells can have profound secondary effects on axonal function and survival.

As a result, it was proposed that such a requirement for glial support by neurons is raised by myelination itself, due to the physical insulation of axons from the extracellular milieu that comes along with this process. Therefore, oligodendrocytes would need to compensate for this separation (Edgar et al., 2009). Authors of studies in *Cnp1*-deficient mice dared to speculate that oligodendrocyte support to axonal function and survival surpassed their myelin-formation functions (Lappe-Siefke et al., 2003). In fact, recent studies suggest that oligodendroglia can provide crucial energy support to axons, through a specialized transporter of lactate (or pyruvate) to the axonal Nodes of Ranvier. The disruption of this transport leads to axon dysfunction and may ultimately lead to neuron deterioration (Lee et al., 2012).

In addition, during degeneration of the neurons occurs fragmentation of this insulating layer. Several molecules are released, such as myelin-associated glycoprotein (MAG), Nogo, and oligodendrocyte myelin glycoprotein (OMgp). Despite some controversy (Lee et al., 2010), this molecules are thought to inhibit axonal outgrowth and recovery after lesion (Cafferty et al., 2010; Chen et al., 2000; Gonzenbach and Schwab, 2008).

1.3.2. SIRT2 in oligodendroglial cells

Although SIRT2 displays ubiquitous expression, it is a highly abundant protein in the adult brain. Within the mouse brain, SIRT2 is expressed in different cellular types, including oligodendrocytes (Li et al., 2007), microglia (Pais et al., 2013), and neurons (Maxwell et al., 2011).

Relatively recent proteomics studies have revealed the presence of SIRT2 in the myelin sheath (Roth et al., 2006). This was further investigated and the results demonstrated that SIRT2 was localized in

oligodendroglial cells, and that it modulated oligodendrocyte differentiation through its tubulin deacetylation activity (Li et al., 2007). It is still not clear how this process is translated into altered cytoplasmic extensions and how it delays differentiation of oligodendrocytes, but the authors suggest that deacetylation could lower microtubule stability, reduce tubulin polymerization, increase depolymerization, or even alter the binding of tubulin to associated proteins, as previously described in other cell types (Robson and Burgoyne, 1989; Hubbert et al., 2002). SIRT2 is positioned at the paranodal myelin in close proximity of axons, from where it may play this role in axo–glial interactions (Li et al., 2007; Southwood et al., 2007).

Conversely, more recent studies establish SIRT2 as facilitator of cell differentiation in CG4 oligodendroglial cells and that Nkx2.2 via HDAC-1 inhibits this process by binding to a specific region on the Sirt2 promoter (Ji et al., 2011). In addition, it was found that mice lacking PLP/DM20, the major CNS myelin protein, exhibit the complete absence of SIRT2 (Werner et al., 2007), thus demonstrating that these Plp1-encoding splice isoforms (in particular, PLP) selectively regulate SIRT2 transport and abundance into the CNS myelin compartment (Zhu et al., 2012). This raises the question of whether SIRT2 could, in turn, contribute to the PLP-dependent neuroprotection provided to axons by oligodendrocytes.

It is clear that the relationship between oligodendroglial SIRT2 and neuronal axon integrity and regeneration upon lesion needs further clarification, in the context of neurodegenerative diseases.

2. AIMS OF THE STUDY

In order to battle against neurodegenerative disorders, for which there are currently no effective therapies, it is crucial to understand the molecular mechanisms underlying these diseases.

There is no doubt about the strong correlation between Sirtuins and PD. In particular, SIRT2 seems to negatively affect neuronal survival in several PD models. The fact that SIRT2 is present not only in neurons, but also in oligodendrocytes, raises questions about its role in axon-glial interactions, and whether modulating levels of this protein in the oligodendroglia could interfere with neuronal axon integrity and regeneration upon lesion. Consequently, SIRT2 could be able to influence axonal regeneration by regulating both neuronal and oligodendroglial functions.

Further investigation in this matter is clearly required, thus leading us to address the role of oligodendroglial SIRT2 in the differentiation and regeneration of dopaminergic neurons.

To this end, our main aims were:

1. To investigate if *in-vivo* changes in oligodendroglial SIRT2 could influence the number of dopaminergic neurons in the SNpc;
2. To assess neurite regeneration in primary cortical cultures, upon overexpression of oligodendroglial SIRT*2* in a scratch lesion model;
3. To explore the role of SIRT2 in the metabolism of OLN-93, an oligodendrocyte cell line.

3. MATERIALS AND METHODS

3.1. Cell cultures

3.1.1. Primary cortical cultures from rat embryos

Preparation of primary cortical cultures was based on the method from Hilgenberg and Smith (2007). After dissection, E18 mouse embryos were decapitated and placed in ice cold Ca^{+2} and Mg^{+2} free Hank's Balanced Salt Solution (CMF-HBSS) (Gibco #14170-088). Tissue pieces corresponding to the cortex were collected into ice-cold CMF under semi-sterile conditions. Briefly, heads were held from the eyes, while scalp was sagittally cut. The skulls were then exposed and released to the side (facilitated by coronal incisions) to expose the brains. After extraction, the brains were transferred to a glass dish, maintained cold by pre-cooled metal disc. After carefully peeling off the meninges, cortices were separated with a sterile needle, cut into small pieces and collected in CMF.

Cortical fragments were centrifuged for 5 minutes at 150g, 4°C. Supernatant was carefully discarded and DNAse I (Roche #04716728001) and trypsin were added to the tube containing the tissue, placed then at 37°C for 10-15 minutes. Extra DNAse and Fetal Bovine Serum (FBS) (PAA, Cölbe, Germany) were added to the mix, in order to inhibit sticking of cells to debris and DNA released from the damaged cells, and to stop the trypsinization reaction, respectively. After centrifugation, using the same settings as before, supernatant was discarded, FBS was added and cells were triturated using a fire-polished glass pipette and the suspension was left still for a few minutes in order to allow debris to sink. The liquid was then transferred to a new 15 ml tube and centrifuged as before. Supernatant was discarded and cells were resuspended in 4-6 ml of Neurobasal medium (Gibco, Invitrogen #21103-049), warmed to 37°C and pre-prepared with the following supplements:

- B27 supplement (Gibco, Invitrogen 50X #17504-044), diluted 1:50
- Penicillin/Streptomycin (P/S) (PAN, Biotech #P06-07100), diluted 1:100
- Transferrin (1mg/mL stock, Sigma #T8158), diluted 1:200
- Glutamine (PAA #M11-004, 0.5mM), diluted 1:400

Cells were counted using Trypan-blue (Gibco, Invitrogen #15250-061), performed by Countess Automated Cell Counter (Invitrogen) and cell density was adjusted to $1x10^6$ per mL in Neurobasal medium. $2.5x10^5$ cells were seeded per well in 24-well cell culture plates (Corning) containing 13Ø coverslips previously coated with poly-L-ornithine (PLO, 100 µg/ mL) (Sigma, #P3655-1G), for immunocytochemistry (ICC) assays. For Western Blot (WB), were seeded 5 or $6x10^5$ cells per well in pre-PLO-coated 12-well cell

culture plates. Cells were incubated at 37°C in humidified, 5% CO_2 incubators. Half volume of medium was refreshed every 3-5 days.

3.1.2. OLN-93 rat oligodendroglia cell line

OLN-93 cells were kindly provided by Dr. Poul Henning Jensen (Department of Biomedicine, Aarhus University, Denmark) and were maintained in Dulbecco's modified Eagle's medium (DMEM) (PAN, Biotech #P04-03550) medium supplemented with 10% FBS (PAA, Cölbe, Germany) and 1% P/S (PAN, Aidenbach, Germany). Cells were grown at 37°C in an atmosphere of 10% CO_2 (Richter-Landsberg and Heinrich, 1996).

$1.5x10^5$ cells were seeded per well in 12-well plates, in order to perform WB assays. For ICC, were seeded $5x10^4$ cells in 24-well plates containing 13Ø coverslips previously coated with poly-L-lysine (PLL) (Sigma, #P1524). For the Seahorse assay, 5000 cells per well were seeded in specific Seahorse XF96 Cell Culture Microplates, previously coated with PLL.

3.2. Lentivirus (LV)

3.2.1. Plasmid preparation

The original FuGW vector, a third generation lentiviral plasmid with a human polyubiquitin promoter-C (hUbC)-driven enhanced green fluorescent protein (EGFP), was a gift from David Baltimore (Caltech, USA) (Lois et al., 2002). From this vector, the hUbC-promoter was deleted by digestion, using the restriction enzymes PacI and BamHI. The insert of interest, rat myelin basic protein (MBP) promoter, specific for oligodendrocytes, was generated by PCR using particular primers, including the PacI-site at the 5´prime end, and the BglII at the 3´prime end of the DNA. (**Fig. 3.2-1 A**).

For the second plasmid (**Fig. 3.2-1 B**), the newly synthesized plasmid was digested using the restriction enzymes AgeI and EcoRI to delete the GFP insert, and the new insert carrying the SIRT2 gene fused with a flag-tag was ligated to the vector using the same enzymes (**Fig. 3.2-1 C**).

In order to prepare the lentivirus, bacterial colonies were grown from a cryovial in liquid 2x LB medium supplemented with 0.2% (v/v) ampicillin. After incubation at 37°C for 16 hours, shaking at 225 rpm, an aliquot was transferred to a larger volume of 2x LB medium containing the antibiotic, in order to further expand bacterial growth. The following day, bacterial cultures were harvested by centrifugation (10 min, 6000g, 4°C) and the plasmid preparation was performed using NucleoBond® PC 2000 (Macherey-Nagel, GmbH & Co. KG, Germany) according to manufacturer's instructions.

An additional precipitation step was necessary in order to increase plasmid purity, by adding 1/10 of the total DNA volume of Sodium Acetate 3M and 2.5x the previous final volume of 100% ethanol. Samples were incubated for 20 min at -30°C and the DNA pelleted by centrifugation (10 min at 15000g, 4°C). Supernatant was discarded and the pellet rinsed 3 times with 70% ethanol, followed by resuspension with 500-700 µL of TE buffer (Lonza, AccuGENE®) according to the size of the pellet.

Plasmid purity was confirmed by spectrometric measurement using the Nanodrop (ND-1000 Spectrometer V3.5.2), and also by DNA digestion using the same restriction enzymes as when the insert was isolated. Dr. Ellen Gerhardt and Christiane Fahlbusch very kindly helped with all the process. Maps of the final plasmids are represented in **Fig. 3.2-2**.

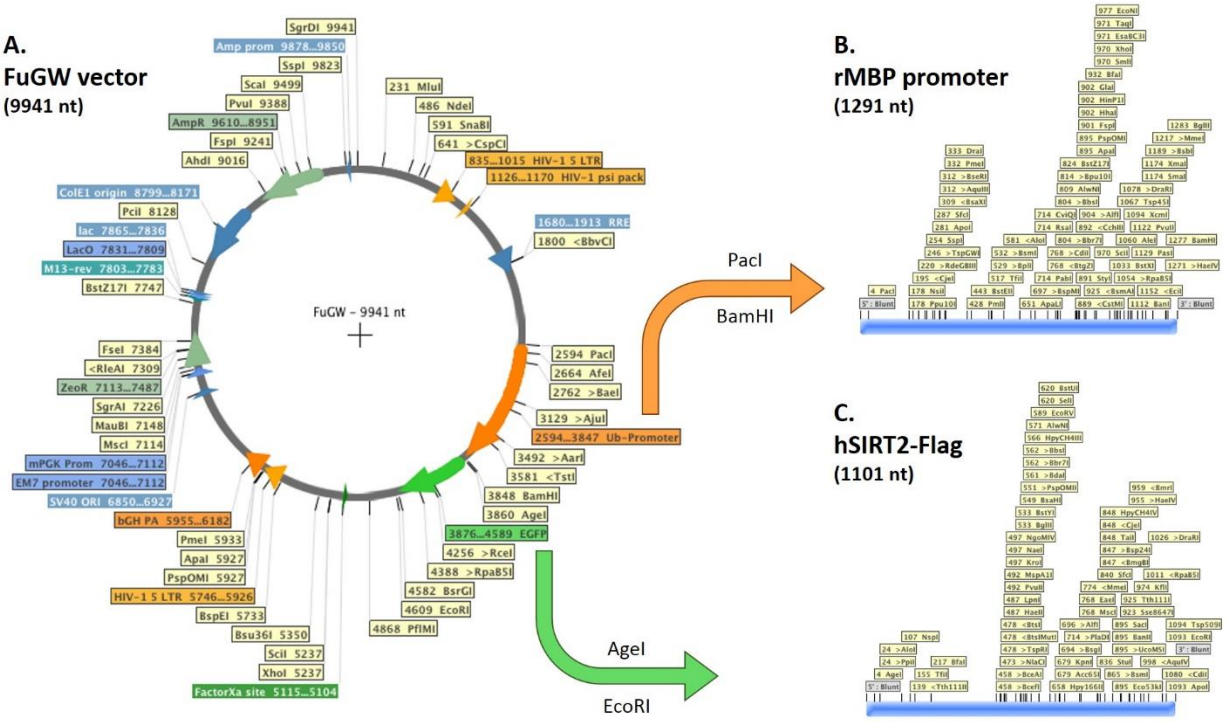

Figure 3.2-1. Schematic representing the construction of the plasmids used in this study. (A) From the original vector FuGW was removed the Ub-promoter (represented in orange) using the restriction enzymes PacI and BamHI, and inserted **(B)** the new rat myelin basic protein (rMBP) promoter. Later, from the newly constructed plasmid, the EGFP site (in green) was removed using AgeI and EcoRI and inserted **(C)** the SIRT2-Flag insert.

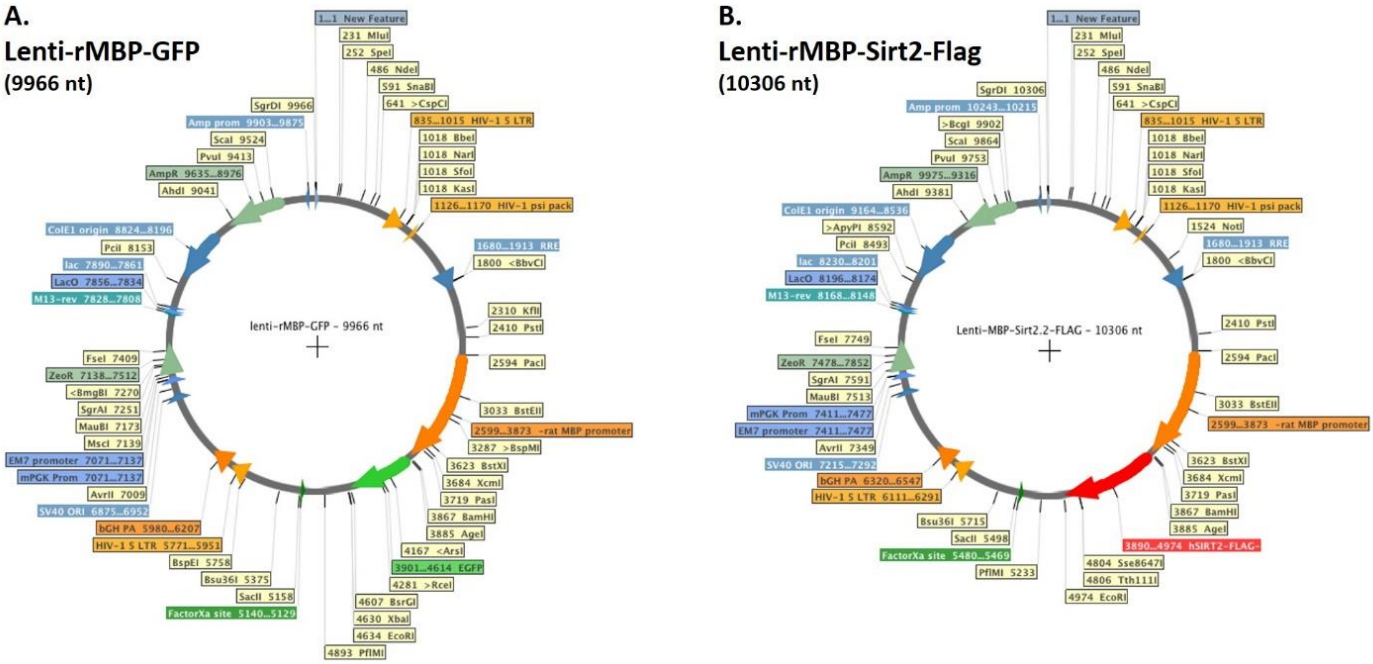

Figure 3.2-2. Maps of the plasmids used in the study. (A) Lentiviral vector expressing GFP (depicted in green) through a rat MBP promoter (in orange). **(B)** Lentiviral vector carrying SIRT2 coupled with a flag tag (in red), with a rat MBP promoter (in orange).

3.2.2. Lentivirus production

In order to produce the lentivirus, HEK-293FT cells were seeded in eight 16 x 15 cm Petri dishes, pre-coated with 0.1% (v/v) Gelatin in ddH_2O, and containing DMEM medium supplemented with 10% FCS, 1% P/S and 1% MEM. 24 hours later, medium was changed to medium containing only 0.02% FCS in DMEM. After around 4h, the Calcium Phosphate Transfection Method was performed (flemingtonlab.com) in order to deliver to the cells 160µg of our plasmid of interest, 144µg of a packing plasmid (Δ8.9) and 57.9µg of an envelope formation plasmid (VSVG) – so that the lentivirus can be created.

16 hours later, medium was changed to Panserin 293A medium (PAN, Invitrogen, #P04-710608) supplemented with 1% P/S and 1% MEM. 72 hours after transfection, the supernatant of the 8 plates was collected for purification. LV were purified and concentrated by using 2 consecutive ultracentrifugation steps. For the first ultracentrifugation procedure, the collected supernatant was distributed among 6 x 38.5mL Beckmann 344058 UC-tubes. From the bottom, 4mL of sterile 20% (w/v) sucrose solution were carefully added to each tube with a Pasteur pipet. The samples were centrifuged at 4°C for 2 h at 20000 rpm, the supernatants were discarded and the pellets were resuspended in 1mL of 1x PBS at 4°C ON. The following day, the 6mL from the resuspended pellets were pulled together in a 13.2mL Beckmann 344059 UC-tube, in which 4mL of Panserin 293A medium were added and 2mL of sterile 20% (w/v) sucrose solution

were carefully added as before. After centrifugation at 4°C for 2h at 26000 rpm, the supernatant was discarded and once the pellet was dry, it was resuspended in 75-85µL of 1xPBS and transferred into a pre-cooled 1.5mL Eppendorf tube. To increase the purity, the virus suspension was centrifuged at 4°C for 3 min at 3000 rpm and the supernatant was finally aliquoted and stored at -80°C.

3.3. *In-vitro* experiments

3.3.1. Infection with LVs

a. Primary cortical cultures

Cells were seeded in either 12 or 24-well plates, depending on the desired experiment. 5 days after seeding, LV particles were diluted 1:100 in Neurobasal medium to facilitate pipetting, and Sirt2-Flag and GFP-carrying LVs were individually added to the wells according to their growth area: 30 µL to 24-well plates and 70 µL to 12-well plates. Some wells were left with no infection.

On the following day, half of the volume was replaced with fresh medium. Cells were maintained for 3 weeks in culture to allow myelination to occur, with half-medium changes every 3-5 days.

b. OLN-93 cell line

Naïve OLN-93 cells (passage 6) were seeded in 2 separate T25 flasks (Corning). When 50% of confluence was reached, 5µL of the LVs used in this study was individually pipetted into the flasks. Cells were replenished with fresh medium on the following day, and used for the experiments after 3 extra passages.

3.3.2. Primary cortical cultures treatment and scratch assay

After 3 weeks of maintenance, cells were treated with 0.005µM of rotenone diluted in Dimethyl sulfoxide (DMSO) (Carl Roth GmbH, Karlsruhe, Germany), a concentration enough to stress cells without killing them. DMSO was used as a control for the Rotenone treatment, diluted in the same proportion in Neurobasal medium.

The cells seeded in the 12-well plates were lysed the next day for WB experiments. For these assays, some of the wells did not receive any treatment.

Scratch assay was performed on cells harvested in the 24-well plates (Tönges et al., 2011). This method is based on the assumption that, upon creation of an artificial gap (the "scratch") on a confluent cell monolayer, the cells on the edge of the newly created gap will attempt to close the gap (Liang et al., 2007). Briefly, cells were submitted to a mechanical transection using a 1 mL pipette tip. Each coverslip was microscopically examined to ensure that the scratch was complete, and cells were maintained for 1-2 days until axonal outgrowth was visible. Afterwards, cells were fixed and ICC was performed.

3.3.3. Cell lysis and protein extraction

Cell medium was aspirated and cells were washed once with 1x Phosphate-Buffered Saline (PBS). 100µL/well of nuclear lysis buffer (50mM Tris pH= 7.5, 2mM EDTA, 0.5M NaCl, 0.1% SDS, 1% NP-40, 1% Deoxycholate, 1x complete protease inhibitor (Roche) in ddH_2O) was added, and culture plates were incubated at 4°C for 10 minutes to facilitate lysis. After scraping, lysates were transferred to a pre-cooled Eppendorf tube, vortexed and kept on ice for 30 min, and then centrifuged at 4°C for 30 min, 15000g. Supernatants were collected to a new pre-cooled Eppendorf tube and either used for protein measurement or stored at -30°C.

3.3.4. Protein quantification

To ensure equal loading of proteins in order to accurately compare protein expression levels in different samples, the Bradford kit was used (BioRad Laboratories GmbH, München, Germany).

In order to obtain an absorbance standard curve, the samples were compared to standard protein samples of known concentrations: 150 µL of the Bradford solution are mixed with 50 µL of the respective standard solution (0, 0.1, 0.25, 0.5, 1, 2, 4 and 6 mg/mL of BSA in bi-distilled water) in triplicates, in a 96-well plate compatible with Infinite® 200 PRO TECAN reader. To obtain protein measurements, 1 µL of each sample of cell lysates is added in triplicates to 49 µL of bi-distilled water, being then mixed with 150 µL of the Bradford solution. Using the Magellan™ data analysis software (Tecan, Switzerland), absorbance was measured at 595 nm and a standard curve is created automatically, calculating sample concentrations (µg/µl) using the following formula: (absorbance- y axis intercept)/slope.

Samples were then prepared for electrophoresis. The protein amount used for samples obtained from primary cortical cells was 10 µg, and 30 µg was used for OLN-93 cell samples.

3.3.5. Western Blotting

Samples were heated to near boiling (5 min at 95°C) in the presence of Laemlli buffer diluted to 1x in protein samples (5x: 125 mM Tris; 4% SDS; 0,5% Bromphenol blue; 4 mM EDTA; 20% Glycerol; 10% β-Mercaptoethanol). This process facilitates denaturation of proteins' secondary and tertiary structures.

Samples were loaded into a polyacrylamide gel (12%), prepared by mixing 24.8% (v/v) separating buffer (150 mM Tris base, 0.4 % (w/v) SDS, pH adjusted to 8.8), 39.6% (v/v) acrylamide/bisacrylamide solution (AppliChem GmbH, Darmstadt, Germany), 0.5% (v/v) TEMED (AppliChem GmbH, Darmstadt, Germany) and 34,6% (v/v) bi-distilled H2O (ddH2O). Ammonium persulfate (APS) (0.5 % v/v) (Schleicher/Schüll bioscience, Keene, USA) was added to initiate the crosslinking. This solution was transferred into a gel cast and leveled by adding 70% (v/v) ethanol, which was removed after polymerization. In these gels, it is necessary to add an upper part with lower acrylamide percentage, in order to stack proteins at the same level before separating them. The stacking gel (7,5 %) is composed of 24,8 % (v/v) stacking buffer (50 mM Tris base, 4 % (w/v) SDS pH adjusted to 6.8 with HCl), 24.8 % (v/v) acrylamide/bisacrylamide, 49.4 % (v/v) ddH2O, 0.5 % (v/v) TEMED and 0,5 % (v/v) APS. After addition of APS, the mixture was overlaid on the separating gel and a gel comb was inserted.

After applying electric voltage, the negatively charged proteins migrate to the positive electrodes, and are therefore separated according to their size: the smaller the protein, the faster it migrates (and vice-versa). Samples and protein ladder (10-250 kDa, BioRad Laboratories, Hercules, CA, USA) were loaded into the gel and ran in Rotiphorese® 10x TBE buffer (Roth GmbH, Karlsruhe, Germany) diluted to 1x in ddH_2O, at 2 steps: 30 minutes at 65 V and at 85-95 V until separation of proteins is complete (around 1h30).

Proteins were then transferred to a 0.2µm nitrocellulose membrane (Trans-Blot® Turbo™ Midi Nitrocellulose Transfer Packs #1704159) using the Trans-Blot® Turbo™ Transfer System. The transference of the proteins from the gel to the membrane was performed at 2.5V and 1A for 30 min.

Membranes were fixed with 0.4% paraformaldehyde (PFA) for 30 min, and transfer was confirmed by staining with Ponceau solution (0.1% (w/v) Ponceau S in 1 mL acetic acid, in ddH2O). Membranes were then blocked for 2-3h at room temperature (RT) with 4% (w/v) Bovine Serum Albumin (BSA) (nzytech #MB04603) in 1x TBS-T (50mM Tris, 150mM NaCl, 0.05% Tween 20, pH=7.5) in order to minimize unspecific bonding upon antibody addition.

Membranes were incubated with primary antibodies in the presence of 4% (w/v) BSA in 1x TBS-T, overnight (ON) at 4°C in agitation, as shown in **table 3.I.** After washing 3 times with 1x TBS-T, membranes were incubated with secondary antibody as shown in **table 3.II**, diluted in 4% (w/v) BSA in 1x TBS-T up to 2 hours. Then, membranes were washed again 3 times with 1x TBS-T and protein detection was made using

the ECL chemiluminescent detection system (Milipore, Billerica, MA, USA) in Fusion FX (Vilber Lourmat). Proteins were quantified using ImageJ software (http://rsbweb.nih.gov/ij/download.html).

3.3.6. Immunocytochemistry

Two weeks after infection, primary cortical cells were fixed with 4% paraformaldehyde (PFA) ON at 4°C. After washing with 1x PBS (10x: 1.37M NaCl, 27mM KCl, 101.4mM $Na_2HPO_4 7.H_2O$, 16.7mM KH_2PO_4, pH= 7.4), cells undergo a retrieval method in order to unmask antigen ligation sites. Citrate buffer (10mM Sodium Citrate, 0.05% Tween 20, pH= 6) was added to each well and warmed up to 80°C, for 15 min. After cooldown to RT, cells were washed 3 times with 1x PBS, permeabilized for 10 min with a solution containing 0.1% (v/v) Triton X-100 (Sigma-Aldrich, St. Louis, MO, USA) in 1xPBS, and blocked with a solution containing 1.5% BSA diluted in 1x PBS for 2 hours.

As for OLN-93 cells, fixation with 4% was performed for 20 min RT, followed by washing with 1x PBS. Then, cells were permeabilized for 20 min with the previously described Triton X-100 containing solution and blocked for 2h with 1.5% BSA in 1x PBS.

All cells are then incubated ON with the primary antibody diluted in the same blocking solution. Antibodies were used as shown in **Table 3.3-1.** On the next day, secondary antibodies were added for 2 hours, as shown in **Table 3.3-2**. Finally, nuclei were stained with Hoechst 33258 (Molecular Probes, Eugene, OR, USA) for 10 minutes, in a ratio of 1:5000 in 1x PBS and rinsed with 1x PBS. Coverslips were removed from the plate and mounted in objective slides using Mowiol. Once dried, were analyzed through fluorescent microscopy.

3.3.7. Fluorescence Microscopy

Olympus IX81-ZDC microscope system (Olympus Germany, Hamburg, Germany) was used in order to acquire images from stained cortical cells by using the Xcellence software. Scratch and axonal projections were visualized with 10x magnification, OLN-93 cells with 20x magnification, and oligodendrocytes with 60x magnification lenses. Lengths of 15 to 30 axonal projections per condition were afterwards measured using the ImageJ software (http://rsbweb.nih.gov/ij/download.html).

3.3.8. Cell metabolism analyzes

Seahorse XFe96 extracellular flux analyzer uses optical sensors in order to simultaneously measure the proton and oxygen levels in a very small volume of media above a monolayer of cultured cells. It measures the rate of oxygen consumption by the cells (OCR), an indicator of mitochondrial respiration. At the same time, cells generate ATP via the oxygen-independent glycolysis, converting glucose to lactate. The Seahorse analyzer measures the extracellular acidification rate (ECAR), given by the indirect measurement of lactic acid produced via the release of protons to the extracellular surrounding medium. Together, OCR and ECAR can provide important insight into the metabolic role of mitochondrial proteins (Ferrick et al., 2008).

Seahorse assays took place on the 5th day after seeding OLN-93 cells. To perform the experiment, 100 mL of DMEM XFe96 Medium was warmed up to 37°C and supplemented with 2mM pyruvate and 2mM glutamine, with pH adjusted to 7.4. For the OCR measurement, 50 mL of this medium was supplemented with additional 10 mM of glucose (Sigma). The drugs necessary for the experiment were diluted in the final supplemented medium according to the following concentrations:

- 2µM of Oligomycin (Sigma, #O4876-25MG), a mitochondrial complex-V inhibitor, allowing the measurement of ATP production and proton leakage;
- 2µM of FCCP, an uncoupling agent responsible for disrupting ATP synthesis, allowing to measure maximal respiration;
- 2µM of Antimycin A plus 5µM of rotenone, mitochondrial complex-III and complex-I inhibitors, respectively, allowing the measurement of spare respiratory capacity of these organelles (**Fig. 3.3-1 A**)**.**

These drugs were added in half of the plate, in ports A, B and C, respectively. On the other half of the plate, compounds necessary for the ECAR measurement were added by the same order, being previously diluted in the medium without glucose, as follows:

- 10mM of glucose, in order to induce glycolysis;
- 2 µM of Oligomycin, in order to stop mitochondrial respiration and measure glycolytic capacity
- 50 mM of 2-deoxy-D-glucose, a glucose molecule that cannot be used for glycolysis, allowing the measurement of glycolytic reserve (**Fig 3.3-1 B**)**.**

The plate with the ports was kept at 37°C in a CO_2-free environment. Meanwhile, plates containing the OLN-93 cells were washed four times with the correspondingly supplemented DMEM XF Medium, and finally 180µL of mediums were added. Cells were then kept at 37°C in a CO_2-free environment. Afterwards,

the drug-containing plate was added to the Seahorse machine in order to start calibration of the sensors, which takes around 30 min to be completed. After calibration was set, the utility plate was replaced with the cell culture plate, and XF assay began. Drugs were automatically injected into the cell culture plate and simultaneous ECAR and OCR measurements were performed.

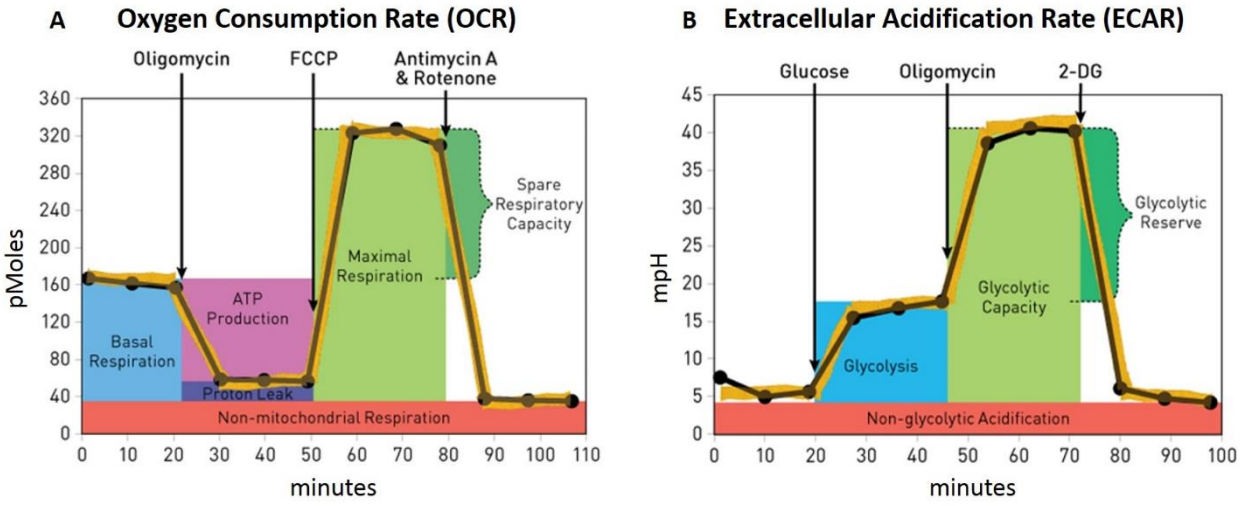

Figure 3.3-1. Illustration of the measurements performed by the Seahorse XFe96 Extracellular Flux analyzer. (A) Oxygen consumption rate (OCR) will represent the mitochondrial respiration state. **(B)** Extracellular acidification rate (ECAR) will portray cell's glycolytic function. (Adapted from https://biophy.uchicago.edu/seahorse.php)

3.3.9. Antibodies used in this study

Primary antibody	*Dilution (WB)*	*Dilution (ICC)*	*Company*	*Raised in*
Anti-CNP	1:500	1:500	Sigma	Rabbit
Anti-Flag	1:3000	1:1000	Sigma	Rabbit
Anti-Flag		1:1000	Stratagene	Mouse
Anti-GAP-43	1:1000		Santa Cruz	Goat
Anti-GFP		1:2000	Antibodies	Rabbit
Anti-GFP	1:2500	1:2000	Roche	Mouse
Anti-Sirt2	1:2500	1:1500	Sigma	Rabbit
Anti- α-synuclein	1:3000		BD Transduction	Mouse
Anti-α-tubulin	1:4000	1:2000	Sigma	Mouse
Anti-acetylated-α-tubulin	1:3000		Cell Signaling Technology	Rabbit
Anti-acetylated-Lysine	1:1000		Cell Signaling Technology	Rabbit

Table 3.3-1. Primary antibodies used in the in-vitro experiments. Different dilutions were used for western blot (WB) and immunocytochemistry (ICC), according to data sheet recommendations.

	Secondary antibody	*Dilution*	*Company*	*Raised in*
For WB	**Anti-mouse**	1:10000	GE Healthcare	Sheep
	Anti-rabbit	1:10000	GE Healthcare	Goat
	Anti-goat	1:10000	Jackson ImmunoResearch	Donkey
For ICC	**anti-mouse IgGAlexa488**	1:1000	Life Technologies - Invitrogen	Donkey
	anti-rabbit IgGAlexa488	1:1000	Life Technologies - Invitrogen	Donkey
	anti-mouse IgG-Alexa568	1:1000	Life Technologies - Invitrogen	Donkey
	anti-rabbit IgG-Alexa568	1:1000	Life Technologies - Invitrogen	Donkey
	anti-rabbit IgG-Alexa568	1:1000	Life Technologies - Invitrogen	Goat

Table 3.3-2. Secondary antibodies used in the in-vitro experiments. Secondary antibodies for immunocytochemistry (ICC) are fluorescent, in contrast to the ones used for western blot (WB).

3.4. *Ex-vivo* experiments

The mouse brains used for *ex-vivo* experiments in this study were kindly handed by Dr. Kathrin Kusch, from the group of Prof. Dr. Klaus-Armin Nave (Department of Neurogenetics, Max-Planck Institute of Experimental Medicine, Göttingen, Germany), after perfusion fixation with 4% PFA.

Wild-type (WT) C57/BL6N mice were used as controls, whereas the conditional knockouts (KO) were generated (unpublished) from animals received from the European Conditional Mouse Mutagenesis Program (EUCOMM) harboring the KO-first allele ($Sirt2^{tm1a(EUCOMM)Wtsi}$) (**Figure 3.4-1**). This KO has a reporter-tagged insertion with conditional potential through the Cre/loxP recombination system (Kos, 2004). In brief, the deletion of the LacZ/neo cassette by crossbreeding to transgenic mice expressing Flp recombinase resulted in the establishment of $Sirt2^{floxed}$ allele (Sirt2 exon 9 flanked by LoxP sites).

For deriving an oligodendrocyte specific conditional KO mice, $Sirt2^{floxed}$ mice were crossbred to $Cnp^{Cre/+}$ mice expressing CRE recombinase specifically in oligodendrocytes and Schwann cells (Lappe-Siefke et al., 2003). Following conditional deletion of the floxed exon by CRE-induced recombination, both protein coding transcripts are predicted to produce a truncated protein product which may be subject to non-sense mediated decay (NMD).

For the neuronal specific conditional KO mice, NEX-Cre was used as a Cre deliver line, expressing the Cre transgene under the control of the NEX promotor (Goebbels et al., 2006). NEX-Cre +/+ have no Cre transgene, thereby being the control ("WT"), and NEX-Cre +/- are the neuronal KO, expressing the Cre transgene.

Figure 3.4-1. Representation of the Sirt2 KO-first allele (Sirt2$^{tm1a(EUCOMM)Wtsi}$). Image from EUCOMM database (http://www.mousephenotype.org/data/genes/MGI:1927664)

3.4.1. Brain sectioning

Brains were transferred to a tube containing 30% sucrose (Roth GmbH, Karlsruhe, Germany) in 1x PBS and kept ON at 4°C until saturation. Excess of sucrose was then removed, and brains were either stored at -80°C or right away sliced.

For sectioning, each brain was placed in a tissue holder with Tissue-Tek® OCT compound (Sakura® Finetek, USA) and 30µm coronal slices were cut using the Leica CM3050S cryostat at -21°C. With the help of a soft brush, sections containing total SNpc were selected between Bregma -2.46mm and -4.04mm (Paxinos and Franklin, 2004). These sections were collected to a 48-well plate filled with 0.2% sodium azide (Carl Roth GmbH, Karlsruhe, Germany) in 1x TBS (50mM Tris, 150mM NaCl, pH= 7.5).

3.4.2. Immunohistochemistry: DAB staining

Free-floating sections were washed 3 times with 1x TBS and incubated for 15 min with a solution containing 3% H2O2 and 40% methanol in 1x TBS, in order to block the activity of endogenous peroxidases. After rinsing 3 times with 1x TBS, slices were blocked for 2h with a solution of 0.3% Triton X-100 and 3% BSA in 1x TBS.

Later, the sections were incubated for 48h at 4°C with the primary antibody (Tyrosine hydroxylase, 1:1000, Merck Millipore) diluted in the same blocking solution. Subsequently, sections were incubated with biotinylated goat anti-rabbit IgG (1:200; Vector Laboratories, Burlingame, CA) for 2 h. This was followed by treatment with Vector avidin–biotin–HRP complex (Vector Standard Elite kit, 1:200; Vector Laboratories) for 2 h. Peroxidase labeling was visualized by 3,3'-diaminobenzidine (DAB) using glucose oxidase. In brief, the development of the staining requires a solution with 25 ml of 0.2 M NaAC at pH=6, 400 µl glucose, 100 µl $(NH_4)_2SO_4$, and the addition of 12.5 mg DAB in 25 ml of ddH_2O. After filtration, glucose oxidase was added to the mix, and the final solution was poured onto the slices for around 2 min, until a brown color was revealed.

After re-washing 3 times with 1x TBS, the slices were placed in an objective slide. After drying, slices were dehydrated in increasing percentages of ethanol, ending in xylol, in order to permanently mount them. Finally, slices were mounted in Entellan® (Merck Millipore).

3.4.3. Stereology

The number of dopaminergic SNpc neurons was assessed by counting the number of TH-positive cells. This was done using the Optical Fractionator, a stereological technique largely used for cell counting (Sterio, 1984), with the StereoInvestigator software (MBF Bioscience, Magdeburg), under the 100x objective lense (Carl Zeiss NEOFLUAR 100x/1.30 Oil 160/), under the Axioskop 2 Zeiss microscope (Jena, Germany). The cell counts carried out with this software are unbiased, since it is not influenced by the size, shape, spatial orientation, and spatial distribution of the cells under study. The equation that the software uses for assessing cell numbers has the following parameters:

$$N = \sum Q^{-} \cdot \frac{t}{h} \cdot \frac{1}{asf} \cdot \frac{1}{ssf}$$

Q^- : Particles counted
t : Section cut thickness
h : Counting frame height
asf : Area sampling fraction
ssf : Section sampling fraction

Blind analysis of the 4 groups of animals was performed by counting TH-positive cells in every 4 slices collected from the mouse brains. Using the software, the region of interest (SNpc) was draw, TH-positive cells were counted at random locations inside the depicted area, and finally the program extrapolated the number of neurons in the total extent of the SNpc. Numbers presented are the estimated population using mean section thickness.

3.5. Statistical analysis

For statistical evaluation of the data, the Graphpad PRISM 7 (San Diego, California, USA) software was used. *Ex-vivo* experiments were performed at least in triplicate. Differences between groups were considered statistically significant according to unpaired t-test. *In-vitro* experiments were performed at least in duplicate, and differences between groups were assessed with one-way ANOVA or two-way ANOVA followed by a parametric multiple comparison test (Tukey's test). Statistical significances for all groups are indicated with *$p<0.05$ and **$p<0.01$.

4. RESULTS

4.1. Neuronal KO of Sirt2 decreases, whereas oligodendroglial Sirt2-KO increases the number of TH+ cells in the mouse brain

Genetic deletion of Sirt2 in the MPTP-mouse model of PD leads to neuroprotection (Liu et al., 2014). Furthermore, in our laboratory, we found that the lack of Sirt2 from the total forebrain affects the development of nigral dopaminergic neurons (Szegő and Outeiro, submitted). This prompted us to explore whether there could be any differences in the number of dopaminergic neurons in this pathway, upon a conditional deletion of Sirt2 in neurons and in the glia, more specifically in oligodendrocytes.

Conditional Sirt2-KO and WT mice were perfused and their brains were extracted and cryopreserved. After coronal sectioning, the number of dopaminergic neurons in the SNpc was assessed by means of stereology after TH immunostaining.

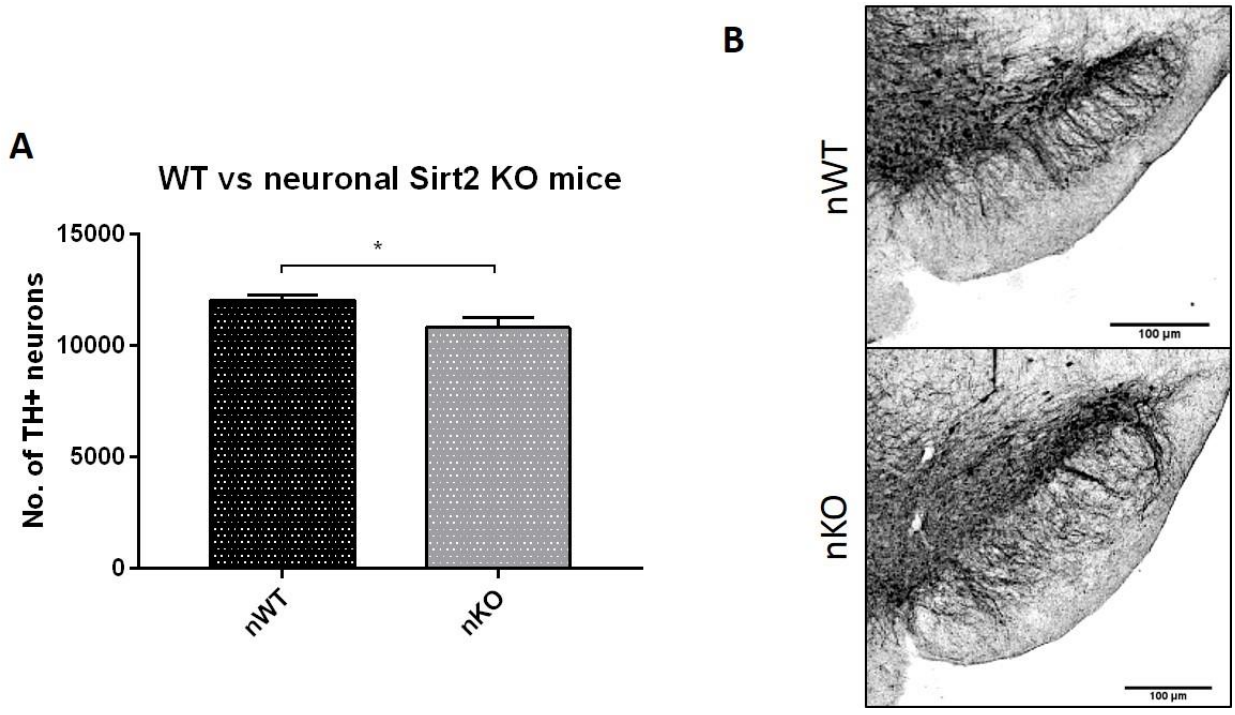

Figure 4.1-1. Deletion of neuronal Sirt2 reduces the number of dopaminergic neurons in mouse brains. (A) Quantification of TH-positive neurons in the SNpc of WT and of neuronal Sirt2-KO mice, using the StereoInvestigator software. Results are expressed as mean ± SD (n=3-4). Statistical analysis was carried out using the unpaired t-test. *p < 0.05. **(B)** Panel shows immunostaining of TH-positive neurons in the SNpc of the referred mouse strains. Scale bar represents 100µM.

We observed that the number of dopaminergic neurons, given by the number of TH-positive cells, is decreased in Sirt2-KO specific for neurons in mice brains, in comparison to WT mice (**Figure 4.1-1**). On the other hand, conditional oligodendroglial Sirt2-KO mice present a higher number of TH-positive cells,

comparing to WT mice of the same group of animals (**Figure 4.1-2**). Given these results, we decided to further explore the role of SIRT2 in oligodendrocytes and its influence on dopaminergic neurons.

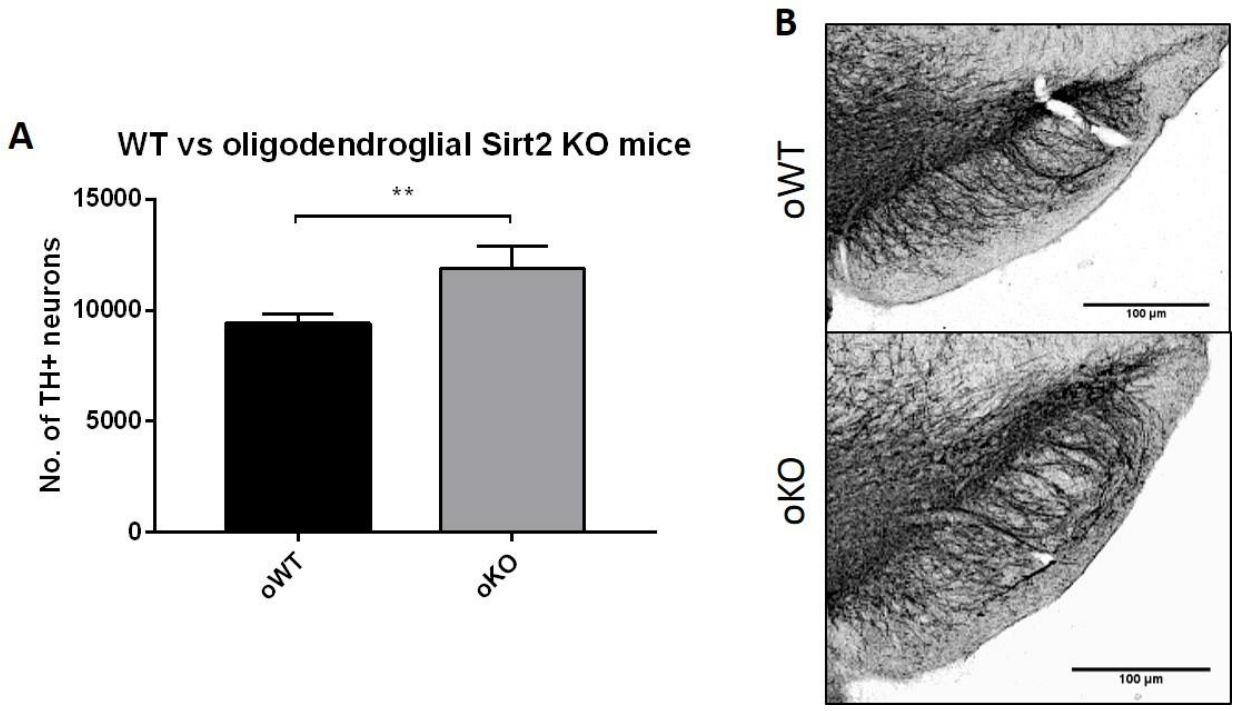

Figure 4.1-2. Deletion of oligodendroglial Sirt2 increases the number of dopaminergic neurons in mouse brains. (A) Quantification of TH-positive neurons in the SNpc of WT and of oligodendroglial Sirt2-KO mice, using the StereoInvestigator software. Results are expressed as mean ± SD (n=3-4). Statistical analysis was carried out using the unpaired t-test. **p < 0.01. **(B)** Panel shows immunostaining of TH-positive neurons in the SNpc of the referred mouse strains. Scale bar represents 100µM.

4.2. SIRT2 overexpression alters oligodendrocyte morphology and total levels of acetylated α-tubulin, but not CNP levels

In order to study the influence of SIRT2 in oligodendrocytes, we decided to use primary cell culture. This mixed-culture represents an excellent model of the brain's complex cellular environment and is therefore very useful to study interactions between neurons and glia.

Primary cortical cultures were infected one week after seeding with LV carrying either Sirt2 with a Flag-tag or GFP, both driven by an oligodendrocyte-specific MBP promoter. Cells were maintained for a total of 3 weeks so that myelination could occur, and then analyzed via fluorescence microscopy or WB assays.

We observed that CNP is present in all cultures, regardless of the infection or treatment performed, meaning that all cultures have myelinating oligodendrocytes (Lappe-Siefke et al., 2003) (**Fig. 4.2-1 A**). In addition, we observed that, even though oligodendrocytes represent a small percentage of cells in these

cultures, modulation of oligodendroglial SIRT2 seems to significantly contribute to the reduction of total levels of acetylated α-tubulin in comparison to the other groups (**Fig. 4.2-1 A, C**).

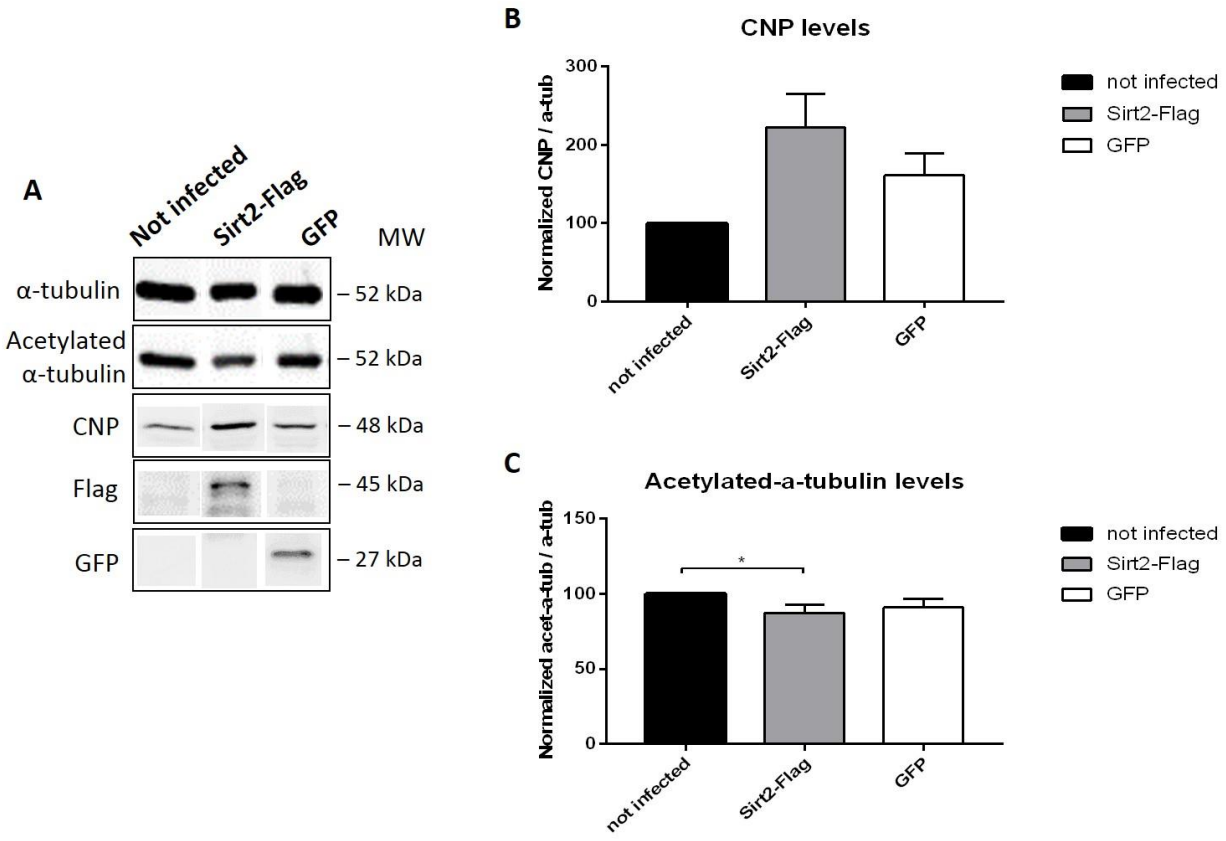

Figure 4.2-1. SIRT2 overexpression affects total acetylated α-tubulin levels but not CNP levels. (A) Representative immunoblot of CNP, Flag and GFP expression. α-tubulin was used as a loading control. **(B)** Quantification of CNP protein levels. CNP/ α-tubulin ratio was determined and all conditions were normalized to not infected cells value. Experiment performed in triplicate. Bars represent mean values ± SD. Statistical analysis was carried out using one-way ANOVA with post-hoc Turkey's test, with no significance between groups ($p>0.05$). **(C)** Quantification of acetylated α-tubulin protein levels. Acetylated α-tubulin/ α-tubulin ratio was determined and all conditions were normalized to not infected cells value. Experiment performed in triplicate. Bars represent mean values ± SD. Statistical analysis was carried out using one-way ANOVA with post-hoc Turkey's test. *$p < 0.05$.

Although cultures infected with MBP-Sirt2-Flag seem to display a tendency towards an increase in CNP levels, in comparison with the other two groups, statistical analysis of this pattern did not reveal a significant difference (**Fig. 4.2-1 B**). On the other hand, analysis through immunofluorescence yielded clear results regarding oligodendrocyte morphology. Cultures infected with MBP-Sirt2-Flag show oligodendrocytes with higher branching and differentiation than the ones in the other two types of cultures (**Fig. 4.2-2**).

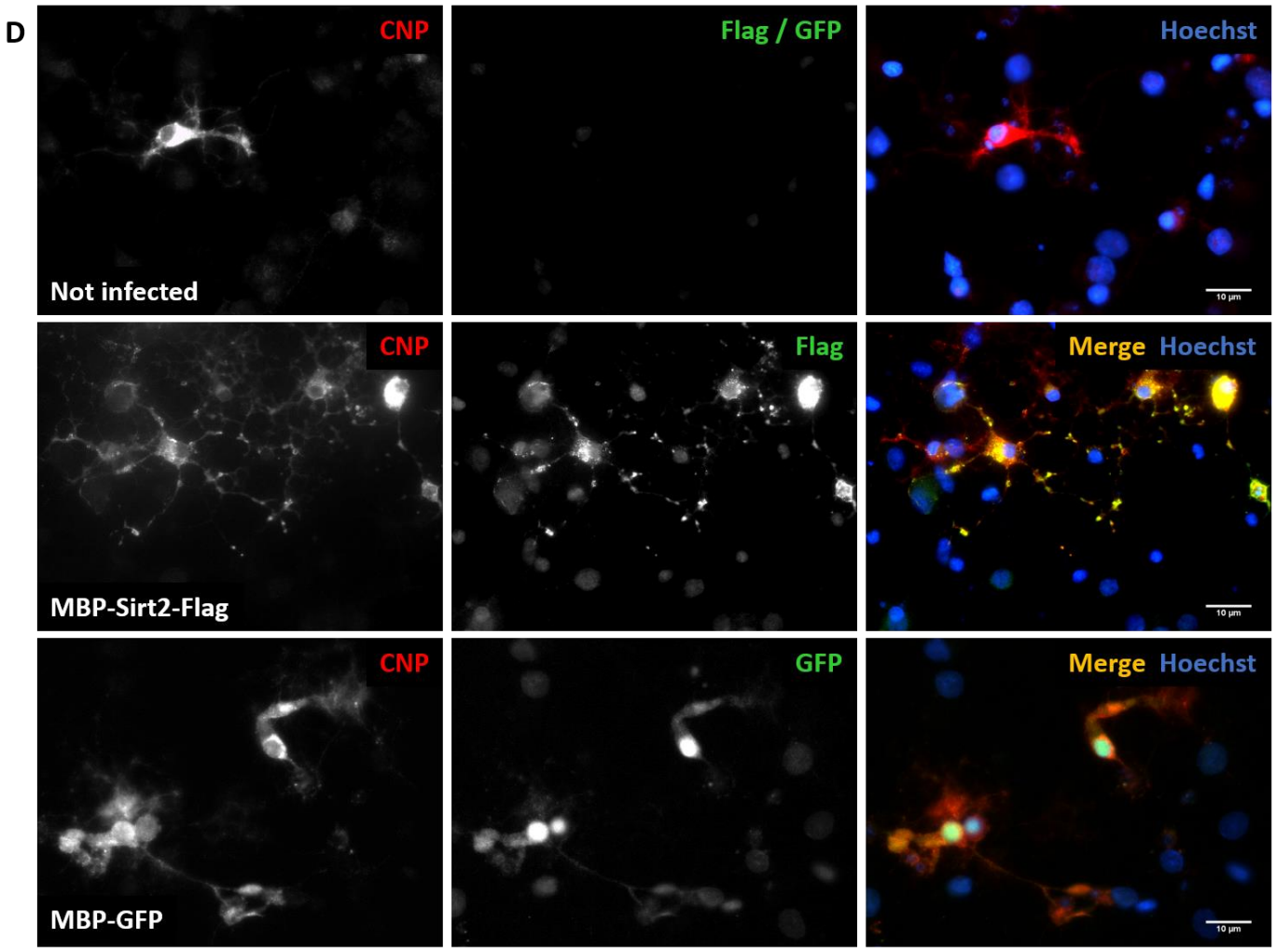

Figure 4.2-2. SIRT2 overexpression affects oligodendrocyte morphology. Representative immunofluorescent images of oligodendrocyte morphology for each condition. Staining for CNP (red), Flag and GFP (green), Hoechst (blue). Yellow color arises when there is an overlay of CNP and Flag or GFP. Scale bar: 10 µm.

4.3. SIRT2 overexpression in oligodendrocytes induces a rotenone-dependent effect on α-synuclein levels, but not on endogenous SIRT2 and GAP-43 levels

Since SIRT2 modulated oligodendroglial morphology, we asked whether this could have an impact on the protection of neurons in the context of neurodegeneration.

The same type of cell cultures was used as before, infected either with MBP-Sirt2-Flag or with GFP. In addition, non-infected cells were used as a control of the infection. To evaluate neuronal survival, 0.5 nM of the mitochondrial complex-I inhibitor rotenone was added to the cultures. DMSO was used as a vehicle control for the rotenone treatment.

We analyzed together the total levels of endogenous SIRT2.1 and SIRT2.2 isoforms, in order to assess any fluctuations in their expression. The form of SIRT2 overexpressed in part of the cultures was not included in this investigation, since its flag-tag increases the molecular weight of the protein and can, therefore, be separated from the other forms (**Fig. 4.3-1 A**). We observed that total endogenous SIRT2 levels seem to have a tendency towards an increase when cell cultures are infected, although this could not be confirmed by statistical analysis (**Fig. 4.3-1 B**). Therefore, infection or treatment of the cells does not seem to significantly interfere with endogenous SIRT2 levels.

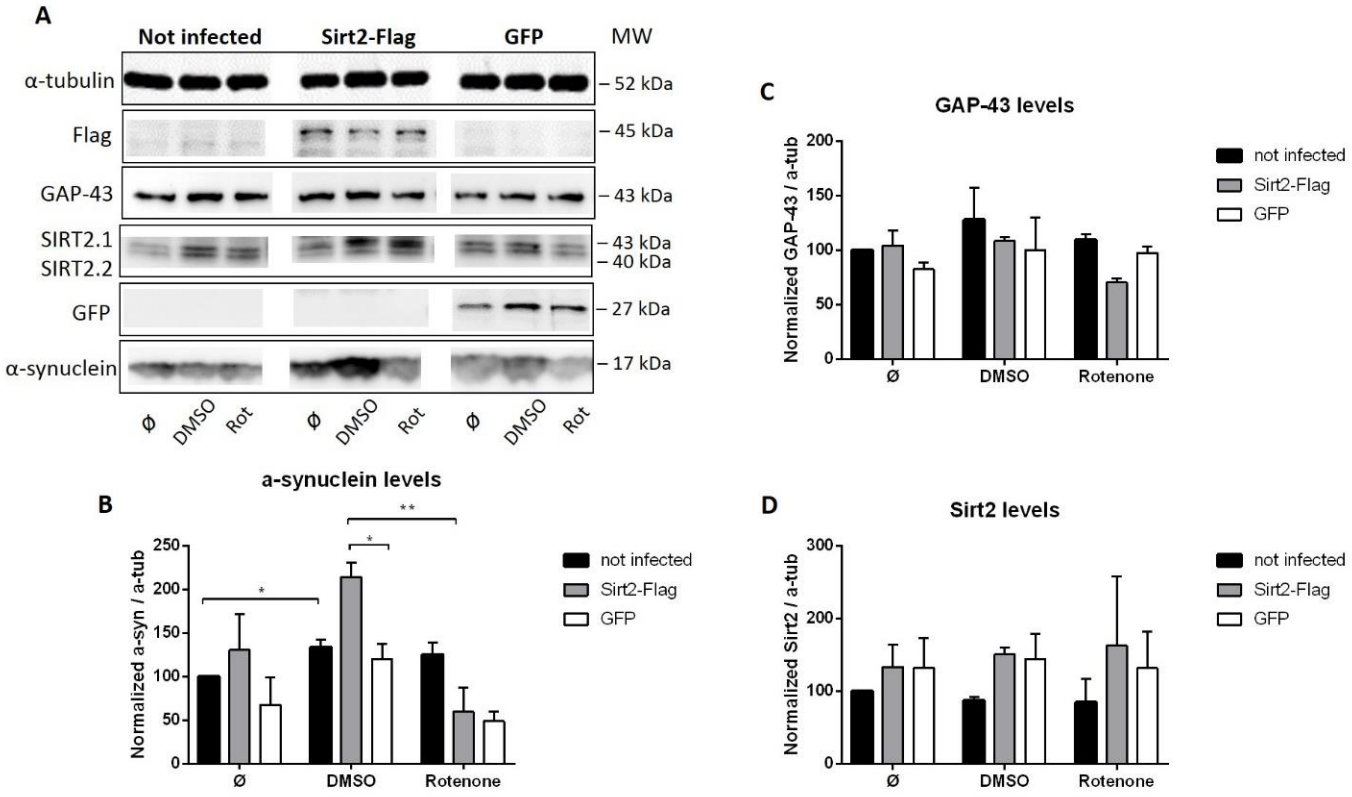

Figure 4.3-1. Oligodendroglial SIRT2 overexpression might have a treatment-dependent impact on α-synuclein levels, but not in endogenous levels of SIRT2 and GAP-43. (A) Representative immunoblot of Flag and GFP expression, along with GAP-43, endogenous isoforms of SIRT2 and α-synudein. α-tubulin was used as a loading control. **(B)** Quantification of SIRT2, **(C)** α-synudein and **(D)** GAP-43 protein levels. Proteins / α-tubulin ratio was determined and all conditions were normalized to non-infected cells under no treatment. Experiment performed in duplicate. Bars represent mean values ± SD. Statistical analysis was carried out using two-way ANOVA with post-hoc Turkey's test. *p<0.05, **p < 0.01.

α-synuclein is a central player in PD (Spillantini et al., 1998). Thus, we decided to analyze whether there were differences in its levels. There are significant differences between treatments: non-infected cultures treated with DMSO express higher amounts of the protein, comparing to the non-treated group;

while the overexpression of SIRT2 in DMSO treated cultures have highly increased levels of α-synuclein comparing to cultures treated with rotenone (**Fig. 4.3-1 A, C**). In summary, rotenone treatment seems to have a tendency to reduce the levels of α-synuclein present in the SIRT2 overexpressing-cultures.

We decided to complement this study by analyzing the levels of GAP-43, in order to investigate whether axonal regeneration could be triggered or inhibited in any of the groups. Although there seems to be a tendency towards the decrease of GAP-43 levels when rotenone is added to cultures overexpressing oligodendroglial SIRT2, no statistical significance was found between the studied groups (**Fig. 4.3-1 A, D**).

4.4. Oligodendroglial SIRT2 overexpression does not influence axonal regeneration in an in-vitro model of PD

Since myelination affects axonal health and therefore the response to stress, we decided to evaluate axonal regeneration utilizing a simple method called scratch assay. We used the same models as before, after treatment with 0.5 nM of rotenone or DMSO. Cultures were fixed 48h after treatment and average neurite length was measured at the scratch site. After statistical analysis of the results, we observed no significant differences between any of the groups (**Fig. 4.4-1**).

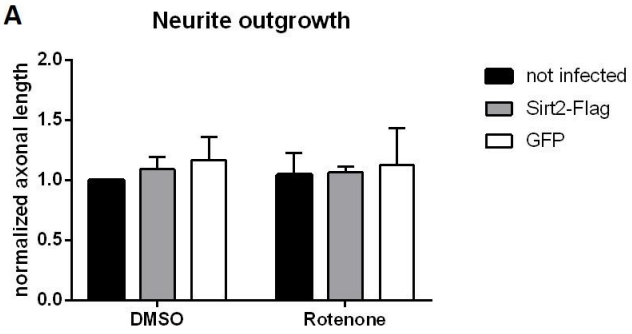

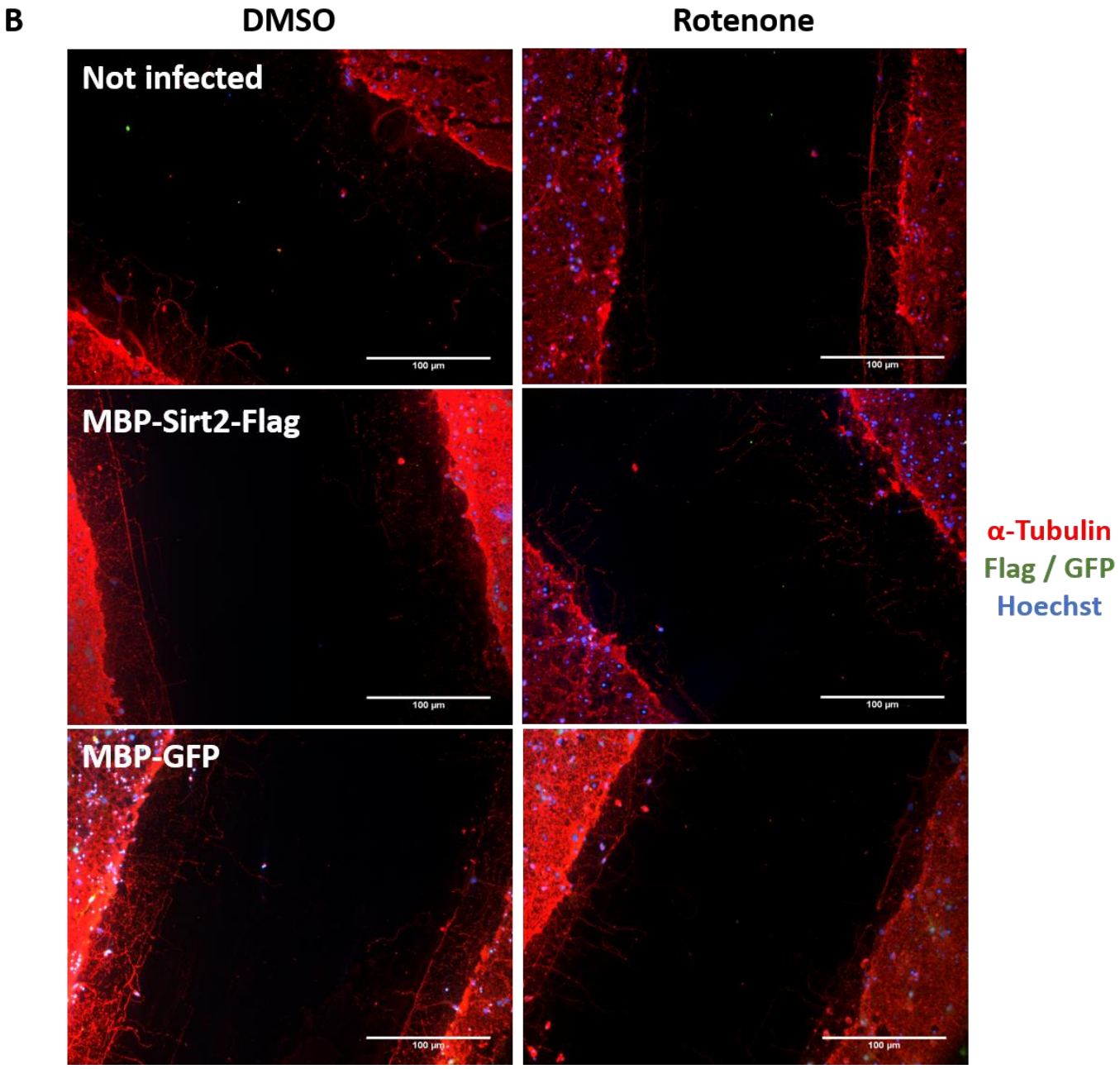

Figure 4.4-1. SIRT2 overexpression in oligodendrocytes does not affect axonal regeneration in-vitro upon rotenone treatment. **(A)** Quantification of axonal lengths, normalized to not-infected cells treated with DMSO. Experiment performed in triplicate. Statistical analysis was carried out using two-way ANOVA with post-hoc Turkey's test, with no significance between groups ($p>0.05$). **(B)** Representative immunofluorescent images of scratch and neurite prolongations, according to the different conditions tested. Scale bar: 100µm.

4.5. SIRT2 overexpression modulates lysine acetylation levels in an oligodendroglial immortalized cell line

The results obtained instigated us to further uncover the effects of SIRT2 in oligodendrocytes. Consequently, we used the permanent oligodendrocyte cell line, OLN-93, to perform these additional assays.

Naïve cells were infected with the same LVs used throughout this study, one carrying Sirt2 with a Flag tag, and the other one carrying GFP, both driven by an oligodendrocyte-specific MBP promoter.

Cells were analyzed under fluorescence microscopy, from which we could confirm the expression of the exogenous proteins (**Fig 4.5-1, 4.5-2 A**). Interestingly, we observed that endogenous SIRT2 seems to be mainly present in the nucleus, although we could also detect it in the cytoplasm. SIRT2-Flag seems to be more evenly distributed between nucleus and cytoplasm. It is noteworthy that this exogenous protein seems to "clump" when distributed in the cytoplasm. However, the altered localization of the protein doesn't seem to affect cell morphology in this cell line. GFP is, as expected, ubiquitously expressed in the cells (**Fig 4.5-1**).

Using WB, we detected levels of both exogenous proteins in the corresponding samples (**Fig. 4.5-2 A**) and we decided to evaluate total levels of acetylated lysines, since SIRT2 acts by deacetylating lysine residues (**Fig. 4.5-2 B**). Statistical analysis could not be implemented, since this experiment was performed only once. Still, WB bands were quantified in order to facilitate interpretation. On a very simplistic approach, SIRT2 overexpression seems to lead towards a decrease in the levels of lysine acetylation of proteins with different molecular weights, corresponding to assigned numbers 1, 2, 3, 6 and 7 (**Figs. 4.5-2 C, D, E, H and I**). It is important to notice that acetylated-lysine (2) corresponds to levels of acetylated-α-tubulin, SIRT2's preferential substrate in neurons. As for the others, SIRT2 does not seem to have an effect on lysine acetylation of proteins corresponding to numbers 4, 5, 8 and 9 (**Figs. 4.5-2 F, G, J and K**). Curiously, lysine acetylation levels of the protein corresponding to number 1 seem highly increased when GFP is expressed (**Fig. 4.5-2 C**).

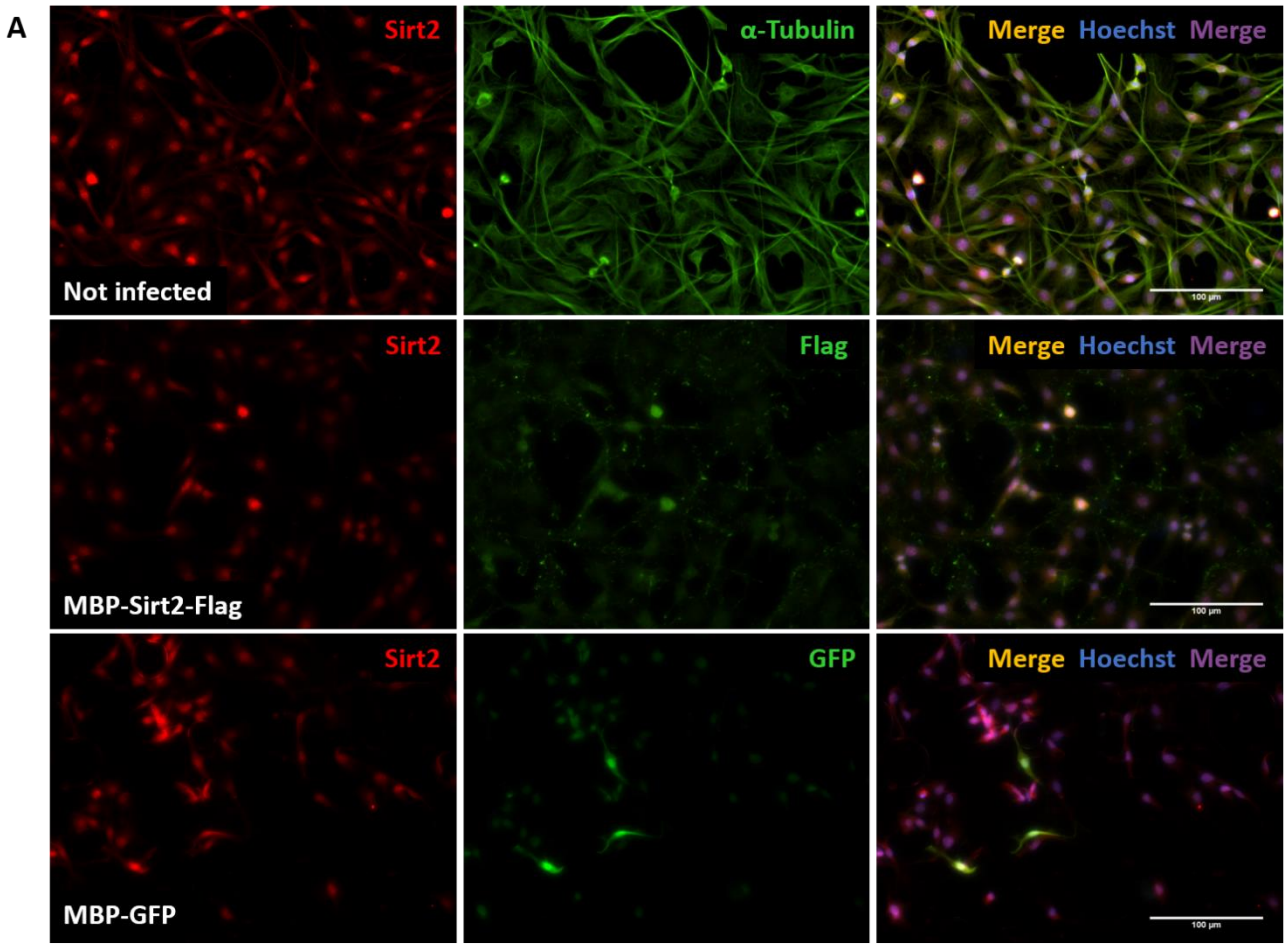

Figure 4.5-1. Endogenous SIRT2 mainly co-localizes with OLN-93 cell nucleus, whereas overexpression of SIRT2-Flag does not affect cell morphology. Representative immunofluorescent images of OLN-93 cells for each condition. Staining for SIRT2 (red), Flag and GFP (green), α-tubulin (green) and Hoechst (blue). Yellow color arises when there is an overlay of SIRT2 and Flag, GFP or α-tubulin. Purple color appears from the overlay of Hoechst and SIRT2. Scale bar: 100 µm.

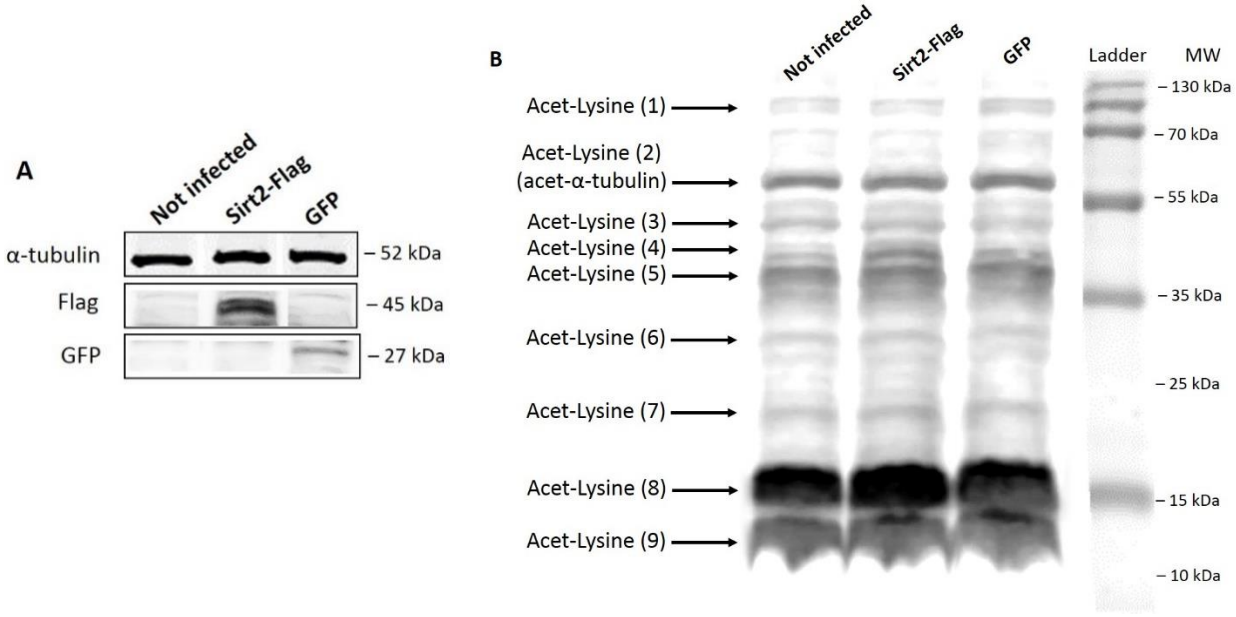

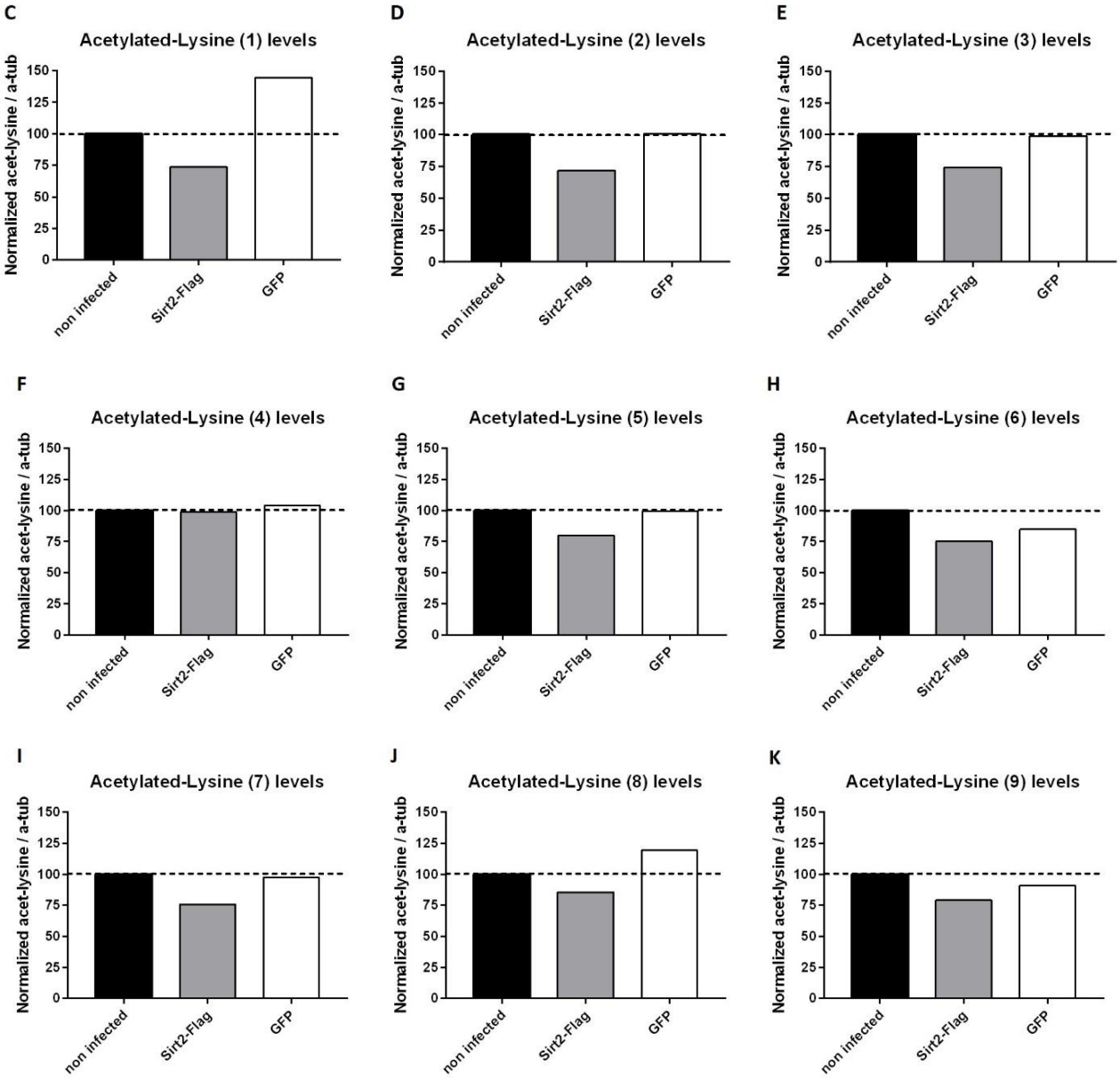

Figure 4.5-2. SIRT2 overexpression modulates acetylation levels of lysine residues, in the OLN-93 oligodendroglial cell line. (A) Representative immunoblots of Flag and GFP, and **(B)** total acetylated-lysine expression in OLN-93 cells. α-tubulin was used as a loading control. **(C-K)** Quantification of bands corresponding to levels of acetylated-lysines in proteins 1-9. "Acetylated-lysine 2" **(D)** matches to acetylated-α-tubulin. N=1. Dashed line added manually in order to facilitate interpretation.

4.6. Overexpression of SIRT2 in OLN-93 cells influences mitochondrial respiration but not glycolytic function

Since it is well known that sirtuins act as deacetylases of enzymes involved in glycolysis, and that oligodendroglial metabolism is crucial in maintaining axonal ion homeostasis (Fünfschilling et al., 2012), we performed the Seahorse assay on OLN-93 cells in order to evaluate their metabolism. We compared the oxygen consumption (OCR) and extracellular acidification (ECAR) rates of cells infected with the same LVs used so far, one carrying Sirt2 with a flag-tag, and the other one carrying GFP.

The baseline measurements were very stable (results not shown), indicating that the assay was working properly. For assessing mitochondrial respiration, three different drugs were injected: oligomycin, which is a mitochondrial complex-V inhibitor, allowing the measurement of ATP production and proton leakage; FCCP, an uncoupling agent that destroys mitochondrial potential and ion gradient across the membrane (which are necessary for ATP production by complex-V), allowing to measure maximal respiration and spare respiratory capacity; and finally a mix of antimycin A and rotenone, mitochondrial complex-III and complex-I inhibitors, respectively, allowing the measurement of non-mitochondrial oxygen production of these organelles. Regarding the OCR measurements, we observed that cells overexpressing SIRT2 seem to have a higher spare respiratory capacity, given by their response to FCCP treatment, comparing to the ones expressing GFP (**Fig. 4.6-1 A**).

To determine their glycolytic functions, cells were previously kept in a medium lacking glucose. Subsequently, glucose was first injected, in order to induce glycolysis, followed by oligomycin, which inhibits mitochondrial ATP production, thereby forcing cells to use glycolysis for ATP generation. As a result, we can measure cellular glycolytic capacity. Finally, by injecting a glucose molecule that cannot be used for glycolysis, 2-deoxy-D-glucose (2-DG), we should be able to measure glycolytic reserve. Interestingly, we did not observe any significant differences between the groups in the ECAR measurements (**Fig. 4.6-1 B**). It is important to mention that 2-DG did not work in these experiments, for reasons we cannot explain at this point.

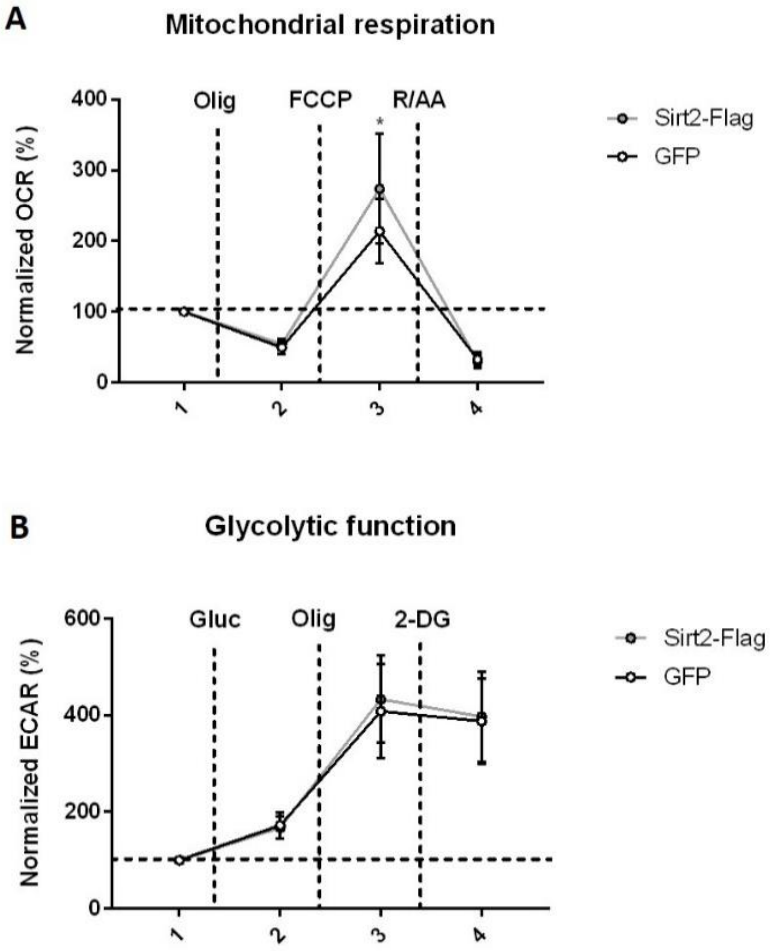

Figure 4.6-1. SIRT2 overexpression in OLN-93 cells alters mitochondrial respiration but not glycolytic function. (A) OCR measurements give a readout for mitochondrial respiration, while **(B)** ECAR measurements represent cells' glycolytic function. Both measurements are normalized to basal respiration and represented as mean ± SD. *x*-axis represents the time-points of measurement. Experiments were performed in triplicate. Statistical analysis was carried out using two-way ANOVA with post-hoc Turkey's test, with no significance between groups. *p<0.05. Oligomycin (Olig); Rotenone plus antimycin A (R/AA); Glucose (Gluc); 2-deoxy-D-glucose (2-DG)

5. DISCUSSION

One of the biggest afflictions in modern days is the increasing prevalence of neurodegenerative diseases among the overall aged populations (World Health Organization, 2006). For that reason, it is crucial to better understand these illnesses, in order to discover efficient therapies against them.

PD is the second most common neurodegenerative disorder (Schlossmacher, 2007), and aging is the major known risk factor for this disorder (Pringsheim et al., 2014). Therefore, aging-related genes are attractive research targets. A good example is the *Sir2* gene, which was found to be a potential mediator of longevity in yeast (Aparicio et al., 1991; Kaeberlein et al., 1999; Sinclair and Guarente, 1997). Mammalian SIR2-like-proteins, or sirtuins (Frye, 2000), are ubiquitous in animals and are thought to regulate a myriad of biological functions (reviews by North and Verdin, 2004; and by Haigis and Sinclair, 2010).

The natural enzymatic activity of sirtuins as cellular protein deacetylases (Finnin et al., 2001) and their presence in several cellular compartments (**Fig. 1.2-1**; reviews by Guarente, 2011; and by Bheda et al., 2016) make them greatly predisposed to interact with a multiplicity of cellular proteins. Sirtuins have lately been described to be highly abundant in the CNS (review by Duan, 2013), in which studies conducted so far point out SIRT1's potentially neuroprotective role in PD models (reviewed by Donmez and Outeiro, 2013), aided by mitochondrial SIRT3, 4 and 5 (Qiu et al., 2010). Interestingly, SIRT2 appears to have the opposite effect: recent investigations show that SIRT2 boosts nigrostriatal damage in animal models of PD, and that this effect can be rescued by deleting the *Sirt2* gene (Liu et al., 2014).

So far, investigations were mainly focused on neuronal SIRT2 (Maxwell et al., 2011), but this protein is also present in other brain cells, such as oligodendrocytes (Li et al., 2007). In addition to their role of neurite myelination (Morell and Quarles, 1999), it is said that oligodendroglia can provide crucial energy support to axons (Lee et al., 2012), thereby suggesting an intricate axonal-glial interaction. Furthermore, myelin fragmentation upon lesion leads to the release of inhibitory molecules, impeding axonal regeneration (Cafferty et al., 2010; Chen et al., 2000; Gonzenbach and Schwab, 2008). Thus, a primary perturbation of myelinating glial cells can have profound secondary effects on axonal function and survival.

In this study, we investigated the role that SIRT2 plays in oligodendrocytes and how relevant this could be in axonal regeneration and PD pathology.

Neuronal KO of Sirt2 decreases, whereas oligodendroglial Sirt2-KO increases the number of TH+ cells in the mouse brain

In our studies we observed that the number of dopaminergic neurons, given by the number of TH-positive cells, is decreased in the SNpc of conditional neuronal Sirt2-KO mice, in comparison to WT mice

(**Fig. 4.1-1**). These results come in agreement with unpublished results from our lab, where the full KO of SIRT2 in mice brains yielded a smaller number of TH-positive cells, comparing with WT mice.
This fact might be simply due, for example, to a basal metabolic mechanism in which SIRT2 could participate. After all, SIRT2 is known to interact with several proteins related to cell metabolism (Gomes et al., 2015).

Conversely, conditional oligodendroglial Sirt2-KO mice presented a higher number of TH-positive cells in the SNpc, comparing to WT mice of the same group of animals (**Fig. 4.1-2**).

Dopaminergic neurons are known to be poorly myelinated cells (Braak and Tredici, 2004), and the SNpc contains mostly dopaminergic neuron's cell bodies, with their axons being projected into the striatum . With this in mind, one could speculate that the effects seen in SNpc dopaminergic neurons on oligodendroglial SIRT2-KO mice would be more related to efficiency in energy support, for example, than in myelination itself.

As previously stated, oligodendroglial SIRT2 was also reported to impede oligodendroglial differentiation through its tubulin deacetylation activity (Li et al., 2007). Therefore, we could wonder if SIRT2 tubulin-deacetylation properties might interfere with the tubulin-stabilization properties of CNP (Bifulco et al., 2002), thereby weakening tubulin-membrane association in oligodendrocytes.

In any of these cases, genetic deletion of the *Sirt2* gene in oligodendrocytes would turn out to be beneficial for oligodendrocyte survival or stabilization, allowing them to support axons.

It would be crucial to observe if this tendency would be maintained in the arborization of the striatal projections, in order to further speculate about SIRT2's oligodendroglial role in the whole nigrostriatal pathway. The evaluation of variances in TH-positive cells in MPTP-treated oligodendroglial Sirt2-KO versus WT mice could also be an exciting approach in order to complement this study. In addition, it could be rather interesting to assess possible differences in the total number of cells in the brains of these mice, by counterstaining slices with Nissl, a classic nucleic acid staining method traditionally used on nervous tissue sections (Fernstrom, 1958).

SIRT2 overexpression affects oligodendrocyte morphology and total levels of acetylated α-tubulin, but not CNP levels

Given these unsettling results, we decided to further explore the role of SIRT2 in oligodendrocytes and its influence in neurons.

We showed that SIRT2, overexpressed in oligodendrocytes, exerts tubulin-deacetylation activity (North et al., 2003) that can be detected by WB, showing a significant decrease in the overall levels of acetylated tubulin (**Fig. 4.2-1 C**). As previously described, CNP is a protein which is also associated with

microtubules, having tubulin-stabilization properties (Bifulco et al., 2002). Therefore, one might speculate that by overexpressing SIRT2, cells would have increased CNP levels in order to compensate this destabilization. On the opposite perspective, by leading to an increase in CNP levels, SIRT2 could facilitate myelin-independent CNP-mediated axonal support (Lappe-Siefke et al., 2003). Cultures infected with MBP-Sirt2-Flag seem to display a tendency towards an increase in CNP levels (**Fig. 4.2-1 B**), but statistical analysis did not reveal a difference between the groups.

As described before, SIRT2 prevents oligodendroglial differentiation through its tubulin deacetylase activity (Li et al., 2007). Curiously, this is not in agreement with our observations, using cortical cell cultures. According to the stages of differentiation of oligodendrocytes (Butts et al., 2008), CNP can be expressed by immature oligodendrocytes already expressing a fully developed arborization, and by mature myelinating oligodendrocytes. Therefore, it is easy to distinguish oligodendrocytes maturation through the complexity of their prolongations. And, in fact, it seems that there is an increase in differentiation and higher branching of oligodendrocytes overexpressing SIRT2, when comparing to naïve or GFP-expressing oligodendrocytes in these cell cultures (**Fig. 4.2-2**), although further tests would be necessary in order to confirm this statement. For example, the Sholl technique (Sholl, 1953), usually used to describe neuronal arbors, could be useful to describe oligodendrocyte arborization. Nonetheless, this would be in agreement with the more recent studies provided by Ji *et al* (2011)**.** This group stated that the beginning of SIRT2 expression in their oligodendrocyte-like cell model goes hand-in-hand with oligodendrocyte differentiation, and that Sirt2 overexpression induced MBP expression and facilitated cell differentiation with the generation of more cytoplasmic processes. Furthermore, it has been speculated if SIRT2 could contribute to the PLP-dependent neuroprotection provided to axons by oligodendrocytes, since PLP is thought to control Sirt2 transport and/or stability in the myelin sheath (Zhu et al., 2012).

With this in mind, it would be interesting to also analyze the levels of MBP and of PLP in SIRT2-overexpressing oligodendrocytes in our cell cultures, in order to obtain more data that would allow us to better interpret these apparently contradictory results. Still, we could once more speculate that SIRT2's apparently beneficial effects in oligodendrocytes of our cellular model would be restricted to oligodendroglia's myelinating capacity, supported by the fact that it seems to correlate mainly with myelin-specific proteins.

SIRT2 overexpression in oligodendrocytes induces a rotenone-dependent effect on α-synuclein levels, but not on endogenous SIRT2 and GAP-43 levels

In order to assess how cells would behave under stress, we treated the different groups of cells with a low dosage of rotenone or DMSO.

We analyzed together the total levels of endogenous SIRT2.1 and SIRT2.2 isoforms, in order to assess any fluctuations in their expression. Statistical analysis did not confirm any significant differences in the overall endogenous levels of SIRT2 in this type of cell culture (**Fig. 4.3-1 A, B**). We can speculate that this might actually be an important result, since SIRT2 overexpression in neurons has been, as mentioned, reported to enhance nigrostriatal damage induced by MPTP-mouse models (Liu et al., 2014). Therefore, the modulation of SIRT2 in oligodendrocytes would theoretically not lead to an increase of SIRT2 in other cell types, minimizing its supposed harmful effects.

Since α-synuclein is deeply associated with neurodegenerative disorders, particularly with PD (Spillantini et al., 1998), we also decided to analyze eventual variations in its levels. Treatment with rotenone reduces the levels of this protein, at least in cells overexpressing oligodendroglial SIRT2 (**Fig. 4.3-1 A, C**).

A recent study demonstrated that rotenone induces the aggregation and phosphorylation of α-synuclein in a calcium-dependent manner, and that aggregated α-synuclein is typically degraded by autophagy, a process which rotenone impairs (Yuan et al., 2015). Therefore, we would expect to observe an increase in the detected levels of α-synuclein in all the rotenone-treated cells, which was not the case. We can merely speculate that the rotenone concentration used in this experiment was not sufficient to induce the same effect as the one observed in the mentioned study. In any case, overexpression of oligodendroglial SIRT2 seems to provoke the biggest difference regarding the levels of α-synuclein between the treatment conditions, from which one could think to be a specific effect of oligodendroglial SIRT2.

Still, as exploring α-synuclein was not the main aim of this project, we did not pursue this experiment in order to be able to explain these results, and this will be further investigated in future studies in the laboratory.

Oligodendroglial SIRT2 overexpression affects axonal regeneration in an in-vitro model of PD

In the context of neurodegeneration, we further tried to evaluate axonal regeneration upon injury, utilizing a simple method called scratch assay. We measured regeneration under previous stress with low dosage of DMSO or rotenone.

We found no significant differences between axonal lengths of any of the groups (**Fig. 4.4-1**). As mentioned before, SIRT2 has been reported to boost nigrostriatal damage induced by MPTP in PD mouse models (Liu et al., 2014). Concomitantly, we were expecting to observe a diminished capacity of axonal regeneration, given by shorter neurite length, in the oligodendroglial SIRT2 overexpressing cells. In stress conditions, upon treatment with rotenone, we were expecting to see an amplification of this effect. Conversely, and given by our data gathered so far on the effect of SIRT2 in oligodendrocyte morphology

(Fig. 4.2-2), we could also expect that overexpression of SIRT2 oligodendrocytes would lead to the increase in axonal support and recovery provided by the intensification of these glial cells maturation. Interestingly, none of these situations was observed, suggesting that oligodendroglial SIRT2 has no effect in axonal regeneration.

In order to support these results obtained within the scratch model, we decided to analyze the levels of neuronal-specific growth-associated protein GAP-43, to investigate whether axonal regeneration could be being triggered or inhibited in any of the groups. No statistical significance was found b etween the studied groups (**Fig. 4.3-1 D**) but there seems to be a tendency towards the decrease of GAP-43 levels when rotenone is added to cultures overexpressing oligodendroglial SIRT2. If, by increasing the number of experiments, this decrease was to be considered significant, it could support the conclusion that SIRT2 overexpression in oligodendrocytes tends to decrease the intrinsic capacity for regeneration of neurons. However, this readout might be an artifact, since it was shown many years ago that GAP-43 is expressed by cells of the O-2A lineage in-vitro, the common progenitor cell for oligodendrocytes and some astrocytes (type-2) (Curtis et al., 1991). Consequently, we could say that the hypothetical decrease in levels of GAP-43 in oligodendroglial SIRT2 overexpressing cells would be due to the apparent improvement in oligodendrocyte differentiation provided by SIRT2 in our cell cultures (**Fig. 4.2-2**).

Nonetheless, the fact that we didn't find statistically significant differences in the levels of GAP-43 seems to be in concordance with our results from the scratch model. However, since rotenone treatment didn't seem to yield any treatment-related effect on GAP-43 levels in the other infection conditions, would be tempting to believe that rotenone truly diminishes neuronal GAP-43 in oligodendroglial SIRT2 overexpressing cells, most likely through its complex-I inhibition-mediated toxicity (Alam and Schmidt, 2002).

SIRT2 overexpression modulates lysine acetylation levels in an oligodendroglial immortalized cell line

The interesting results obtained so far instigated us to further uncover the effects of SIRT2 in oligodendrocytes, using a permanent oligodendrocyte cell line, OLN-93.

In this line, endogenous SIRT2 seemed to be mainly present in the nucleus, although we could also detect it in the cytoplasm. In cells overexpressing SIRT2-Flag, the exogenous protein seemed to be more evenly distributed between nucleus and cytoplasm. Noteworthy, it seemed to form some sort of "clumps" when distributed in the cytoplasm. GFP expression upon infection was ubiquitously distributed along cells. (**Fig. 4.5-1**). In this cell line, SIRT2 overexpression doesn't seem to alter morphology, but it could be that we don't see that change simply due to the density of plated cells.

Since SIRT2 acts by deacetylating lysine residues (Yang and Seto, 2008), we decided to evaluate the levels of the total spectrum of acetylated lysines (**Fig. 4.5-2 B-K**). Although we could not carry out any statistical analysis, since the experiment was performed only once, we could observe what seems to be a tendency for SIRT2 to target several proteins, given by the different molecular weights, and deacetylate their lysine residues.

As mentioned, SIRT2 targets preferentially α-tubulin (North et al., 2003), and therefore is worth mentioning that levels of acetylated α-tubulin seem to be decreased in SIRT2 overexpressing cultures (**Fig. 4.5-2 D**), meaning that SIRT2 is exerting its normal tubulin-deacetylase functions in oligodendrocytes.

Overexpression of SIRT2 in OLN-93 cells influences mitochondrial respiration but not glycolytic function

Currently, SIRT2 has also been implicated in the regulation of several metabolic pathways in mammals, being referred to as a fuel-sensing molecule that adapts its expression and activity according to cell's energetic state (Gomes et al., 2015). Since SIRT2 seemed to display a tendency towards deacetylating lysine residues of several proteins, we speculated if some of these could be related with cell metabolism. Therefore we decided to investigate whether SIRT2 overexpression could influence cell respiratory capacity (OCR) and glycolytic function (ECAR), as measured by the Seahorse assay.

Regarding the OCR measurements, we observed that cells overexpressing SIRT2 seem to have a higher spare respiratory capacity, given by their response to FCCP treatment, comparing to the ones expressing GFP (**Fig. 4.6-1 A**). We might therefore speculate that SIRT2 could provide significant benefits in oligodendrocyte mitochondrial respiration. For example, SIRT2 has been shown to deacetylate peroxisome proliferator-activated receptor gamma (PPARγ) coactivator 1-alpha (PCG-1α) (Krishnan et al., 2012), mediating mitochondrial biogenesis (Wu et al., 1999); and also to upregulate antioxidant enzyme expression with consequent reduction of cellular ROS levels, by deacetylating forkhead box O3a (FOXO3a) (Wang et al., 2007). In theory, both these interactions would be beneficial in cells with such a high energy demands as oligodendrocytes (Harris and Attwell, 2012).

As for their glycolytic functions, given by the ECAR measurements, we could not observe any significant differences between the groups (**Fig. 4.6-1 B**). Oligodendrocytes have recently been described to survive in-vivo by aerobic glycolysis, which leads to the production of lactate used by axons for mitochondrial ATP generation (Fünfschilling et al., 2012). SIRT2 is known to deacetylate PEPCK1 (Jiang et al., 2011), the catalyst of the first committed and rate-limiting step of gluconeogenesis by converting oxaloacetate into phosphoenolpyruvate (Hanson and Reshef, 1997). By increasing its stability under conditions of glucose deprivation, SIRT2 is suggested to enhance PEPCK1-mediated gluconeogenesis,

particularly during times of energy limitation. Therefore, we would expect to see some differences in cells' glycolytic functions, but this was not observed.

Since cultured cells can have different metabolic profiles per se, this phenomena still needs to be further investigated. In order to confirm any of these theories, we would need to confirm the presence of all these proteins in oligodendroglial cells. So, we cannot discard the hypothesis that these pathways might not work in the same way in oligodendrocytes, and that other players could be in the game.

6. CONCLUDING REMARKS

In this study, we attempted to elucidate the role that SIRT2 plays in oligodendrocytes and how relevant this could be in axon regeneration and PD pathology.

Using a permanent oligodendroglial cell line, OLN-93, we learned that SIRT2 seems to be more present in the nucleus, although also in the cytoplasm, and that it seems to exert its deacetylase action upon lysine residues of several proteins, including α-tubulin. Perhaps some of these proteins are involved in the regulation of oligodendrocyte metabolism – at least, it seems like SIRT2 overexpressing cells display increased mitochondrial maximal respiratory capacity. In contrast, SIRT2 does not modify glycolytic functions in these cell types.

Using a more complex cell model, the mixed culture of cortical cells, we aimed to assess the influence of oligodendroglial SIRT2 in neuronal regeneration. Upon SIRT2 overexpression in oligodendrocytes, in these cultures, we could also detect α-tubulin-deacetylation activity, a tubulin destabilization process that we hypothesized that might interfere with the tubulin-stabilization properties of oligodendroglial CNP. Here we observed a tendency to the increase in CNP levels, which we could interpret in two distinct ways. On one hand, SIRT2 could weaken tubulin-membrane association in oligodendrocytes, leading to a compensatory mechanism of CNP overexpression. On the other hand, SIRT2 could facilitate CNP-mediated axonal support, independent of myelination. In addition, SIRT2 seems to increase oligodendrocyte differentiation and branching in cortical cell cultures.

Since sporadic PD patients commonly present defects in mitochondrial complex-I, we tried to mimic this stress by treating cells with rotenone. Endogenous levels of SIRT2 and GAP-43 did not have a treatment-dependent change, but levels of α-synuclein were greatly reduced by treatment with rotenone in oligodendroglial SIRT2 overexpressing cultures. Finally, we evaluated axonal regeneration upon lesion, via the scratch assay, but SIRT2 had no effect on neurite length in the treatment conditions, in concordance with our GAP-43 results.

The information obtained using our cell models tells us that SIRT2 might play an important role in oligodendrocytes, distinct from the deleterious effect it is thought to have in neurons. However, ultimately, cell models are just small and particular reproductions of reality. That is why it is necessary to perform studies in *in-vivo* models, much more realistic representations of the whole panoply of interactions in the brain.

According to our initial studies in mouse brains, the number of dopaminergic neurons in the SNpc is slightly diminished upon genetic deletion of neuronal Sirt2, suggesting a that SIRT2 might have basal beneficial role in neuron survival, most likely related with cell metabolism. However, the number of

dopaminergic neurons in the SNpc drastically increases when Sirt2 is conditionally deleted in oligodendrocytes. This leads us to conclude that, although SIRT2 might really have potentially beneficial effects in oligodendrocytes *in-vitro* and, eventually, *in-vivo* in other brain areas, oligodendroglial SIRT2 is not helpful in the maintenance and support of dopaminergic neurons in the SNpc.

Additional experiments would be necessary to complement these studies on the role of oligodendroglial SIRT2, especially when it comes to neurodegenerative disorders. Nevertheless, all of these experimental procedures open doors to a bigger understanding of the SIRT2-mediated axonal-glia interaction, and hopefully could instigate additional investigation in the context of PD and other brain-affecting illnesses, culminating in the development of novel strategies for therapeutic intervention.

REFERENCES

Abe, N., and Cavalli, V. (2008). Nerve injury signaling. Curr. Opin. Neurobiol. *18*, 276–283.

Aigner, L., and Caroni, P. (1993). Depletion of 43-kD growth-associated protein in primary sensory neurons leads to diminished formation and spreading of growth cones. J. Cell Biol. *123*, 417–429.

Aigner, L., Arber, S., Kapfhammer, J.P., Laux, T., Schneider, C., Botteri, F., Brenner, H.-R., and Caroni, P. (1995). Overexpression of the neural growth-associated protein GAP-43 induces nerve sprouting in the adult nervous system of transgenic mice. Cell *83*, 269–278.

Alam, M., and Schmidt, W.J. (2002). Rotenone destroys dopaminergic neurons and induces parkinsonian symptoms in rats. Behav. Brain Res. 136, 317–324.

Alim, M.A., Ma, Q.-L., Takeda, K., Aizawa, T., Matsubara, M., Nakamura, M., Asada, A., Saito, T., Kaji, H., Yoshii, M., et al. (2004). Demonstration of a role for alpha-synuclein as a functional microtubule-associated protein. J. Alzheimers Dis. JAD 6, 435-442-449.

Albani, D., Polito, L., Batelli, S., De Mauro, S., Fracasso, C., Martelli, G., Colombo, L., Manzoni, C., Salmona, M., Caccia, S., et al. (2009). The SIRT1 activator resveratrol protects SK-N-BE cells from oxidative stress and against toxicity caused by alpha-synuclein or amyloid-beta (1-42) peptide. J. Neurochem. *110*, 1445–1456.

Aparicio, O.M., Billington, B.L., and Gottschling, D.E. (1991). Modifiers of position effect are shared between telomeric and silent mating-type loci in S. cerevisiae. Cell *66*, 1279–1287.

Baumann, N., and Pham-Dinh, D. (2001). Biology of oligodendrocyte and myelin in the mammalian central nervous system. Physiol. Rev. *81*, 871–927.

Bellou, V., Belbasis, L., Tzoulaki, I., Evangelou, E., and Ioannidis, J.P.A. (2016). Environmental risk factors and Parkinson's disease: An umbrella review of meta-analyses. Parkinsonism Relat. Disord. *23*, 1–9.

Bendotti, C., Servadio, A., and Samanin, R. (1991). Distribution of GAP-43 mRNA in the brain stem of adult rats as evidenced by in situ hybridization: localization within monoaminergic neurons. J. Neurosci. *11*, 600–607.

Benowitz, L.I., and Routtenberg, A. (1997). GAP-43: an intrinsic determinant of neuronal development and plasticity. Trends Neurosci. *20*, 84–91.

Bernheimer, H., Birkmayer, W., Hornykiewicz, O., Jellinger, K., and Seitelberger, F. (1973). Brain dopamine and the syndromes of Parkinson and Huntington Clinical, morphological and neurochemical correlations. J. Neurol. Sci. *20*, 415–455.

Betarbet, R., Sherer, T.B., MacKenzie, G., Garcia-Osuna, M., Panov, A.V., and Greenamyre, J.T. (2000). Chronic systemic pesticide exposure reproduces features of Parkinson's disease. Nat. Neurosci. *3*, 1301–1306.

Bheda, P., Jing, H., Wolberger, C., and Lin, H. (2016). The Substrate Specificity of Sirtuins. Annu. Rev. Biochem. 85, 405–429.

Bifulco, M., Laezza, C., Stingo, S., and Wolff, J. (2002). 2',3'-Cyclic nucleotide 3'-phosphodiesterase: A membrane-bound, microtubule-associated protein and membrane anchor for tubulin. Proc. Natl. Acad. Sci. U. S. A. 99, 1807–1812.

Borland, M.K., Trimmer, P.A., Rubinstein, J.D., Keeney, P.M., Mohanakumar, K.P., Liu, L., and Bennett, J.P. (2008). Chronic, low-dose rotenone reproduces Lewy neurites found in early stages of Parkinson's disease, reduces mitochondrial movement and slowly kills differentiated SH-SY5Y neural cells. Mol. Neurodegener. *3*, 1–12.

Braak, H., and Tredici, K.D. (2004). Poor and protracted myelination as a contributory factor to neurodegenerative disorders. Neurobiol. Aging *25*, 19–23.

Bradl, M., and Lassmann, H. (2010). Oligodendrocytes: biology and pathology. Acta Neuropathol. (Berl.) *119*, 37–53.

Brunelle, J.K., and Letai, A. (2009). Control of mitochondrial apoptosis by the Bcl-2 family. J. Cell Sci. *122*, 437–441.

Butts, B.D., Houde, C., and Mehmet, H. (2008). Maturation-dependent sensitivity of oligodendrocyte lineage cells to apoptosis: implications for normal development and disease. Cell Death Differ. *15*, 1178–1186.

Cafferty, W.B.J., Duffy, P., Huebner, E., and Strittmatter, S.M. (2010). MAG and OMgp Synergize with Nogo-A to Restrict Axonal Growth and Neurological Recovery after Spinal Cord Trauma. J. Neurosci. *30*, 6825–6837.

Chen, M.S., Huber, A.B., van der Haar, M.E., Frank, M., Schnell, L., Spillmann, A.A., Christ, F., and Schwab, M.E. (2000). Nogo-A is a myelin-associated neurite outgrowth inhibitor and an antigen for monoclonal antibody IN-1. Nature *403*, 434–439.

Coppedè, Fabio (2012). Genetics and Epigenetics of Parkinson's Disease, Genetics and Epigenetics of Parkinson's Disease. Sci. World J. Sci. World J. *2012*, *2012*, e489830.

Curtis, R., Hardy, R., Reynolds, R., Spruce, B.A., and Wilkin, G.P. (1991). Down-regulation of GAP-43 During Oligodendrocyte Development and Lack of Expression by Astrocytes In Vivo: Implications for Macroglial Differentiation. Eur. J. Neurosci. *3*, 876–886.

Daubner, S.C., Le, T., and Wang, S. (2011). Tyrosine Hydroxylase and Regulation of Dopamine Synthesis. Arch. Biochem. Biophys. *508*, 1–12.

Dauer, W., and Przedborski, S. (2003). Parkinson's disease: mechanisms and models. Neuron *39*, 889–909.

Denu, J.M. (2005). The Sir2 family of protein deacetylases. Curr. Opin. Chem. Biol. *9*, 431–440.

DiMauro, S., and Schon, E.A. (2003). Mitochondrial respiratory-chain diseases. N. Engl. J. Med. *348*, 2656–2668.

Donmez, G., and Outeiro, T.F. (2013). SIRT1 and SIRT2: emerging targets in neurodegeneration: SIRT1 and SIRT2 in neurodegeneration. EMBO Mol. Med. *5*, 344–352.

Donmez, G., Arun, A., Chung, C.-Y., McLean, P.J., Lindquist, S., and Guarente, L. (2012). SIRT1 protects against α-synuclein aggregation by activating molecular chaperones. J. Neurosci. Off. J. Soc. Neurosci. *32*, 124–132.

Duan, W. (2013). Sirtuins: from metabolic regulation to brain aging. Front. Aging Neurosci. *5*.

Edgar, J.M., McLaughlin, M., Werner, H.B., McCulloch, M.C., Barrie, J.A., Brown, A., Faichney, A.B., Snaidero, N., Nave, K.-A., and Griffiths, I.R. (2009). Early ultrastructural defects of axons and axon–glia junctions in mice lacking expression of Cnp1. Glia *57*, 1815–1824.

Fedorow, H., Tribl, F., Halliday, G., Gerlach, M., Riederer, P., and Double, K.L. (2005). Neuromelanin in human dopamine neurons: Comparison with peripheral melanins and relevance to Parkinson's disease. Prog. Neurobiol. *75*, 109–124.

Fernstrom, R.C. (1958). A Durable Nissl Stain for Frozen and Paraffin Sections. Stain Technol. *33*, 175–176.

Ferrick, D.A., Neilson, A., and Beeson, C. (2008). Advances in measuring cellular bioenergetics using extracellular flux. Drug Discov. Today *13*, 268–274.

Finnin, M.S., Donigian, J.R., and Pavletich, N.P. (2001). Structure of the histone deacetylase SIRT2. Nat. Struct. Mol. Biol. *8*, 621–625.

Frye, R.A. (2000). Phylogenetic Classification of Prokaryotic and Eukaryotic Sir2-like Proteins. Biochem. Biophys. Res. Commun. *273*, 793–798.

Fünfschilling, U., Supplie, L.M., Mahad, D., Boretius, S., Saab, A.S., Edgar, J., Brinkmann, B.G., Kassmann, C.M., Tzvetanova, I.D., Möbius, W., et al. (2012). Glycolytic oligodendrocytes maintain myelin and long-term axonal integrity. Nature.

Gal, J., Bang, Y., and Choi, H.J. (2012). SIRT2 interferes with autophagy-mediated degradation of protein aggregates in neuronal cells under proteasome inhibition. Neurochem. Int. *61*, 992–1000.

Gelb DJ, Oliver E, and Gilman S (1999). Diagnostic criteria for Parkinson Disease. Arch. Neurol. *56*, 33–39.

Glorioso, C., Oh, S., Douillard, G.G., and Sibille, E. (2011). Brain molecular aging, promotion of neurological disease and modulation by sirtuin 5 longevity gene polymorphism. Neurobiol. Dis. 41, 279–290.

Goebbels, S., Bormuth, I., Bode, U., Hermanson, O., Schwab, M.H., and Nave, K.-A. (2006). Genetic targeting of principal neurons in neocortex and hippocampus of NEX-Cre mice. Genes. N. Y. N 2000 44, 611–621.

Gomes, P., Fleming Outeiro, T., and Cavadas, C. (2015). Emerging Role of Sirtuin 2 in the Regulation of Mammalian Metabolism. Trends Pharmacol. Sci. *36*, 756–768.

Gonzenbach, R.R., and Schwab, M.E. (2008). Disinhibition of neurite growth to repair the injured adult CNS: Focusing on Nogo. Cell. Mol. Life Sci. *65*, 161–176.

Greenamyre, J.T., Betarbet, R., and Sherer, T.B. (2003). The rotenone model of Parkinson's disease: genes, environment and mitochondria. Parkinsonism Relat. Disord. *9*, *Supplement 2*, 59–64.

Guarente, L. (2011). The Logic Linking Protein Acetylation and Metabolism. Cell Metab. *14*, 151–153.

Haaxma, C.A., Bloem, B.R., Borm, G.F., Oyen, W.J.G., Leenders, K.L., Eshuis, S., Booij, J., Dluzen, D.E., and Horstink, M.W.I.M. (2007). Gender differences in Parkinson's disease. J. Neurol. Neurosurg. Amp Psychiatry *78*, 819–824.

Haigis, M.C., and Sinclair, D.A. (2010). Mammalian Sirtuins: Biological Insights and Disease Relevance. Annu. Rev. Pathol. Mech. Dis. *5*, 253–295.

Hanson, R.W., and Reshef, L. (1997). Regulation of phosphoenolpyruvate carboxykinase (GTP) gene expression. Annu. Rev. Biochem. *66*, 581–611.

Hardy, J. (2010). Genetic Analysis of Pathways to Parkinson Disease. Neuron 68, 201–206.

Harris, J.J., and Attwell, D. (2012). The energetics of CNS white matter. J. Neurosci. Off. J. Soc. Neurosci. *32*, 356–371.

Hilgenberg, L.G.W., and Smith, M.A. (2007). Preparation of Dissociated Mouse Cortical Neuron Cultures. J. Vis. Exp. JoVE.

Hornykiewicz, O. (1998). Biochemical aspects of Parkinson's disease. Neurology 51, S2–S9.

Hubbert, C., Guardiola, A., Shao, R., Kawaguchi, Y., Ito, A., Nixon, A., Yoshida, M., Wang, X.-F., and Yao, T.-P. (2002). HDAC6 is a microtubule-associated deacetylase. Nature *417*, 455–458.

Inoue, T., Hiratsuka, M., Osaki, M., Yamada, H., Kishimoto, I., Yamaguchi, S., Nakano, S., Katoh, M., Ito, H., and Oshimura, M. (2007). SIRT2, a tubulin deacetylase, acts to block the entry to chromosome condensation in response to mitotic stress. Oncogene *26*, 945–957.

Ivy, J.M., Hicks, J.B., and Klar, A.J.S. (1985). Map Positions of Yeast Genes SIR1, SIR3 and SIR4. Genetics *111*, 735–744.

Ivy, J.M., Klar, A.J., and Hicks, J.B. (1986). Cloning and characterization of four SIR genes of Saccharomyces cerevisiae. Mol. Cell. Biol. *6*, 688–702.

Jankovic, J. (2008). Parkinson's disease: clinical features and diagnosis. J. Neurol. Neurosurg. Psychiatry *79*, 368–376.

Ji, S., Doucette, J.R., and Nazarali, A.J. (2011). Sirt2 is a novel in vivo downstream target of Nkx2.2 and enhances oligodendroglial cell differentiation. J. Mol. Cell Biol. *3*, 351–359.

Jiang, W., Wang, S., Xiao, M., Lin, Y., Zhou, L., Lei, Q., Xiong, Y., Guan, K.-L., and Zhao, S. (2011). Acetylation regulates gluconeogenesis by promoting PEPCK1 degradation via recruiting the UBR5 ubiquitin ligase. Mol. Cell *43*, 33–44.

Jw, L., Eb, L., and I, I. (1983). MPTP-induced parkinsonism in human and non-human primates--clinical and experimental aspects. Acta Neurol. Scand. Suppl. *100*, 49–54.

Kaeberlein, M., McVey, M., and Guarente, L. (1999). The SIR2/3/4 complex and SIR2 alone promote longevity in Saccharomyces cerevisiae by two different mechanisms. Genes Dev. *13*, 2570–2580.

Kalivendi, S.V., Cunningham, S., Kotamraju, S., Joseph, J., Hillard, C.J., and Kalyanaraman, B. (2004). Alpha-synuclein up-regulation and aggregation during MPP+-induced apoptosis in neuroblastoma cells: intermediacy of transferrin receptor iron and hydrogen peroxide. J. Biol. Chem. *279*, 15240–15247.

Keane, P.C., Kurzawa, M., Blain, P.G., Morris, C.M., Keane, P.C., Kurzawa, M., Blain, P.G., and Morris, C.M. (2011). Mitochondrial Dysfunction in Parkinson's Disease. Park. Dis. *2011*, e716871.

Kim, H.-S., Vassilopoulos, A., Wang, R.-H., Lahusen, T., Xiao, Z., Xu, X., Li, C., Veenstra, T.D., Li, B., Yu, H., et al. (2011). SIRT2 Maintains Genome Integrity and Suppresses Tumorigenesis through Regulating APC/C Activity. Cancer Cell *20*, 487–499.

Kos, C.H. (2004). Cre/loxP system for generating tissue-specific knockout mouse models. Nutr. Rev. 62, 243–246.

Kowall, N.W., Hantraye, P., Brouillet, E., Beal, M.F., McKee, A.C., and Ferrante, R.J. (2000). MPTP induces alpha-synuclein aggregation in the substantia nigra of baboons. Neuroreport 11, 211–213.

Krishnan, J., Danzer, C., Simka, T., Ukropec, J., Walter, K.M., Kumpf, S., Mirtschink, P., Ukropcova, B., Gasperikova, D., Pedrazzini, T., et al. (2012). Dietary obesity-associated Hif1 activation in adipocytes restricts fatty acid oxidation and energy expenditure via suppression of the Sirt2-NAD+ system. Genes Dev. *26*, 259–270.

Kuzuhara, S., Mori, H., Izumiyama, N., Yoshimura, M., and Ihara, Y. (1988). Lewy bodies are ubiquitinated. Acta Neuropathol. (Berl.) 75, 345–353.

Langston, J.W., Ballard, P., Tetrud, J.W., and Irwin, I. (1983). Chronic Parkinsonism in humans due to a product of meperidine-analog synthesis. Science *219*, 979–980.

Lappe-Siefke, C., Goebbels, S., Gravel, M., Nicksch, E., Lee, J., Braun, P.E., Griffiths, I.R., and Nave, K.-A. (2003). Disruption of Cnp1 uncouples oligodendroglial functions in axonal support and myelination. Nat. Genet. *33*, 366–374.

Lee, H.-J., Shin, S.Y., Choi, C., Lee, Y.H., and Lee, S.-J. (2002). Formation and Removal of α-Synuclein Aggregates in Cells Exposed to Mitochondrial Inhibitors. J. Biol. Chem. 277, 5411–5417.

Lee, J.J., Ham, J.H., Lee, P.H., and Sohn, Y.H. (2015). Gender Differences in Age-Related Striatal Dopamine Depletion in Parkinson's Disease. J. Mov. Disord. *8*, 130–135.

Lee, J.K., Geoffroy, C.G., Chan, A.F., Tolentino, K.E., Crawford, M.J., Leal, M.A., Kang, B., and Zheng, B. (2010). Assessing Spinal Axon Regeneration and Sprouting in Nogo-, MAG-, and OMgp-Deficient Mice. Neuron *66*, 663–670.

Lee, Y., Morrison, B.M., Li, Y., Lengacher, S., Farah, M.H., Hoffman, P.N., Liu, Y., Tsingalia, A., Jin, L., Zhang, P.-W., et al. (2012). Oligodendroglia metabolically support axons and contribute to neurodegeneration. Nature *487*, 443–448.

Li, W., Zhang, B., Tang, J., Cao, Q., Wu, Y., Wu, C., Guo, J., Ling, E.-A., and Liang, F. (2007). Sirtuin 2, a Mammalian Homolog of Yeast Silent Information Regulator-2 Longevity Regulator, Is an Oligodendroglial Protein That Decelerates Cell Differentiation through Deacetylating -Tubulin. J. Neurosci. *27*, 2606–2616.

Liang, C.-C., Park, A.Y., and Guan, J.-L. (2007). In vitro scratch assay: a convenient and inexpensive method for analysis of cell migration in vitro. Nat. Protoc. *2*, 329–333.

Liu, L., Arun, A., Ellis, L., Peritore, C., and Donmez, G. (2014). SIRT2 enhances 1-methyl-4-phenyl-1,2,3,6-tetrahydropyridine (MPTP)-induced nigrostriatal damage via apoptotic pathway. Front. Aging Neurosci. *6*.

Lois, C., Hong, E.J., Pease, S., Brown, E.J., and Baltimore, D. (2002). Germline transmission and tissue-specific expression of transgenes delivered by lentiviral vectors. Science *295*, 868–872.

Lucin, K.M., and Wyss-Coray, T. (2009). Immune Activation in Brain Aging and Neurodegeneration: Too Much or Too Little? Neuron *64*, 110–122.

Luthi-Carter, R., Taylor, D.M., Pallos, J., Lambert, E., Amore, A., Parker, A., Moffitt, H., Smith, D.L., Runne, H., Gokce, O., et al. (2010). SIRT2 inhibition achieves neuroprotection by decreasing sterol biosynthesis. Proc. Natl. Acad. Sci. *107*, 7927–7932.

Maswood, N., Young, J., Tilmont, E., Zhang, Z., Gash, D.M., Gerhardt, G.A., Grondin, R., Roth, G.S., Mattison, J., Lane, M.A., et al. (2004). Caloric restriction increases neurotrophic factor levels and attenuates neurochemical and behavioral deficits in a primate model of Parkinson's disease. Proc. Natl. Acad. Sci. U. S. A. *101*, 18171–18176.

Maxwell, M.M., Tomkinson, E.M., Nobles, J., Wizeman, J.W., Amore, A.M., Quinti, L., Chopra, V., Hersch, S.M., and Kazantsev, A.G. (2011). The Sirtuin 2 microtubule deacetylase is an abundant neuronal protein that accumulates in the aging CNS. Hum. Mol. Genet. *20*, 3986–3996.

Michan, S., and Sinclair, D. (2007). Sirtuins in mammals: insights into their biological function. Biochem. J. *404*, 1–13.

Mizuno, Y., Sone, N., and Saitoh, T. (1987). Effects of 1-Methyl-4-Phenyl-1,2,3,6-Tetrahydropyridine and 1-Methyl-4-Phenylpyridinium Ion on Activities of the Enzymes in the Electron Transport System in Mouse Brain. J. Neurochem. *48*, 1787–1793.

Morell, P., Quarles, R.H. Myelin Formation, Structure and Biochemistry. In: Siegel GJ, Agranoff BW, Albers RW, et al., editors. Basic Neurochemistry: Molecular, Cellular and Medical Aspects. 6th edition. Philadelphia: Lippincott-Raven (1999). Chapter 4. Available from: http://www.ncbi.nlm.nih.gov/books/NBK20402/

Nagatsu, T., and Sawada, M. (2006). Cellular and Molecular Mechanisms of Parkinson's Disease: Neurotoxins, Causative Genes, and Inflammatory Cytokines. Cell. Mol. Neurobiol. *26*, 779–800.

Nave, K.-A., and Trapp, B.D. (2008). Axon-Glial Signaling and the Glial Support of Axon Function. Annu. Rev. Neurosci. *31*, 535–561.

North, B.J., and Verdin, E. (2004). Sirtuins: Sir2-related NAD-dependent protein deacetylases. Genome Biol *5*, 224.

North, B.J., Marshall, B.L., Borra, M.T., Denu, J.M., and Verdin, E. (2003). The human Sir2 ortholog, SIRT2, is an NAD+-dependent tubulin deacetylase. Mol. Cell *11*, 437–444.

Orth, M., and Schapira, A.H.V. (2002). Mitochondrial involvement in Parkinson's disease. Neurochem. Int. *40*, 533–541.

Outeiro, T.F., Kontopoulos, E., Altmann, S.M., Kufareva, I., Strathearn, K.E., Amore, A.M., Volk, C.B., Maxwell, M.M., Rochet, J.-C., McLean, P.J., et al. (2007). Sirtuin 2 inhibitors rescue alpha-synuclein-mediated toxicity in models of Parkinson's disease. Science 317, 516–519.

Outeiro, T.F., Marques, O., and Kazantsev, A. (2008). Therapeutic role of sirtuins in neurodegenerative disease. Biochim. Biophys. Acta BBA - Mol. Basis Dis. 1782, 363–369

Pais, T.F., Szeg\Ho, É.M., Marques, O., Miller-Fleming, L., Antas, P., Guerreiro, P., de Oliveira, R.M., Kasapoglu, B., and Outeiro, T.F. (2013). The NAD-dependent deacetylase sirtuin 2 is a suppressor of microglial activation and brain inflammation. EMBO J. *32*, 2603–2616.

Pallàs, M., Pizarro, J.G., Gutierrez-Cuesta, J., Crespo-Biel, N., Alvira, D., Tajes, M., Yeste-Velasco, M., Folch, J., Canudas, A.M., Sureda, F.X., et al. (2008). Modulation of SIRT1 expression in different neurodegenerative models and human pathologies. Neuroscience *154*, 1388–1397.

Pandya, M., Kubu, C.S., and Giroux, M.L. (2008). Parkinson disease: Not just a movement disorder. Cleve. Clin. J. Med. 75, 856–864.

Park, S., Mori, R., and Shimokawa, I. (2013). Do sirtuins promote mammalian longevity?: A Critical review on its relevance to the longevity effect induced by calorie restriction. Mol. Cells 35, 474–480.

Parkinson, J. (1817). The shaking palsy. Sherwood Neely Jones Lond.

Paxinos, G., and Franklin, K.B.J. (2004). The Mouse Brain in Stereotaxic Coordinates (Gulf Professional Publishing).

Pringsheim, T., Jette, N., Frolkis, A., and Steeves, T.D.L. (2014). The prevalence of Parkinson's disease: A systematic review and meta-analysis: PD PREVALENCE. Mov. Disord. *29*, 1583–1590.

Przedborski, S., Jackson-Lewis, V., Naini, A.B., Jakowec, M., Petzinger, G., Miller, R., and Akram, M. (2001). The parkinsonian toxin 1-methyl-4-phenyl-1, 2, 3, 6-tetrahydropyridine (MPTP): a technical review of its utility and safety. J. Neurochem. *76*, 1265–1274.

Qiu, X., Brown, K.V., Moran, Y., and Chen, D. (2010). Sirtuin regulation in calorie restriction. Biochim. Biophys. Acta *1804*, 1576–1583.

Rack, J.G.M., VanLinden, M.R., Lutter, T., Aasland, R., and Ziegler, M. (2014). Constitutive Nuclear Localization of an Alternatively Spliced Sirtuin-2 Isoform. J. Mol. Biol. *426*, 1677–1691.

Reyes, J.F., Rey, N.L., Bousset, L., Melki, R., Brundin, P., and Angot, E. (2014). Alpha-synuclein transfers from neurons to oligodendrocytes. Glia *62*, 387–398.

Richter-Landsberg, C., and Heinrich, M. (1996). OLN-93: a new permanent oligodendroglia cell line derived from primary rat brain glial cultures. J. Neurosci. Res. *45*, 161–173.

Robson, S.J., and Burgoyne, R.D. (1989). Differential localisation of tyrosinated, detyrosinated, and acetylated alpha-tubulins in neurites and growth cones of dorsal root ganglion neurons. Cell Motil. Cytoskeleton *12*, 273–282.

Roth, A.D., Ivanova, A., and Colman, D.R. (2006). New observations on the compact myelin proteome. Neuron Glia Biol. *2*, 15–21.

Saijo, K., and Glass, C.K. (2011). Microglial cell origin and phenotypes in health and disease. Nat. Rev. Immunol. *11*, 775–787.

Schapira, A.H.V. (1998). Human complex I defects in neurodegenerative diseases. Biochim. Biophys. Acta BBA-Bioenerg. *1364*, 261–270.

Schemies, J., Uciechowska, U., Sippl, W., and Jung, M. (2010). NAD+-dependent histone deacetylases (sirtuins) as novel therapeutic targets. Med. Res. Rev. *30*, 861–889.

Schlossmacher, M.G. (2007). 8 a-Synuclein and Synucleinopathies. Dement. 2 30, 186.

Schlossmacher, M.G., Frosch, M.P., Gai, W.P., Medina, M., Sharma, N., Forno, L., Ochiishi, T., Shimura, H., Sharon, R., Hattori, N., et al. (2002). Parkin localizes to the Lewy bodies of Parkinson disease and dementia with Lewy bodies. Am. J. Pathol. 160, 1655–1667.

Sherer, T.B., Betarbet, R., Testa, C.M., Seo, B.B., Richardson, J.R., Kim, J.H., Miller, G.W., Yagi, T., Matsuno-Yagi, A., and Greenamyre, J.T. (2003). Mechanism of toxicity in rotenone models of Parkinson's disease. J. Neurosci. *23*, 10756–10764.

Sherwood, C.C., Stimpson, C.D., Raghanti, M.A., Wildman, D.E., Uddin, M., Grossman, L.I., Goodman, M., Redmond, J.C., Bonar, C.J., Erwin, J.M., et al. (2006). Evolution of increased glia–neuron ratios in the human frontal cortex. Proc. Natl. Acad. Sci. 103, 13606–13611

Sholl, D.A. (1953). Dendritic organization in the neurons of the visual and motor cortices of the cat. J. Anat. *87*, 387–406.1.

Sinclair, D.A., and Guarente, L. (1997). Extrachromosomal rDNA circles--a cause of aging in yeast. Cell *91*, 1033–1042.

Sofroniew, M.V., and Vinters, H.V. (2010). Astrocytes: biology and pathology. Acta Neuropathol. (Berl.) *119*, 7–35.

Southwood, C.M., Peppi, M., Dryden, S., Tainsky, M.A., and Gow, A. (2007). Microtubule Deacetylases, SirT2 and HDAC6, in the Nervous System. Neurochem. Res. *32*, 187–195.

Spillantini, M.G., Crowther, R.A., Jakes, R., Cairns, N.J., Lantos, P.L., and Goedert, M. (1998). Filamentous α-synuclein inclusions link multiple system atrophy with Parkinson's disease and dementia with Lewy bodies. Neurosci. Lett. *251*, 205–208.

Stemberger, S., Poewe, W., Wenning, G.K., and Stefanova, N. (2010). Targeted overexpression of human α-synuclein in oligodendroglia induces lesions linked to MSA -like progressive autonomic failure. Exp. Neurol. *224*, 459–464.

Sterio, D.C. (1984). The unbiased estimation of number and sizes of arbitrary particles using the disector. J. Microsc. *134*, 127–136.

Sulzer, D. (2007). Multiple hit hypotheses for dopamine neuron loss in Parkinson's disease. Trends Neurosci. *30*, 244–250.

Tönges, L., Planchamp, V., Koch, J.-C., Herdegen, T., Bähr, M., and Lingor, P. (2011). JNK Isoforms Differentially Regulate Neurite Growth and Regeneration in Dopaminergic Neurons In Vitro. J. Mol. Neurosci. *45*, 284–293.

Uhl, G.R., Hedreen, J.C., and Price, D.L. (1985). Parkinson's disease Loss of ineurons from the ventral tegmental area contralateral to therapeutic surgical lesions. Neurology *35*, 1215–1215.

Vaquero, A. (2006). SirT2 is a histone deacetylase with preference for histone H4 Lys 16 during mitosis. Genes Dev. *20*, 1256–1261.

Verma, M., Vats, A., and Taneja, V. (2015). Toxic species in amyloid disorders: Oligomers or mature fibrils. Ann. Indian Acad. Neurol. 18, 138–145.

Wakabayashi, K., Engelender, S., Yoshimoto, M., Tsuji, S., Ross, C.A., and Takahashi, H. (2000). Synphilin-1 is present in Lewy bodies in Parkinson's disease. Ann. Neurol. 47, 521–523.

Wakabayashi, K., Tanji, K., Mori, F., and Takahashi, H. (2007). The Lewy body in Parkinson's disease: molecules implicated in the formation and degradation of alpha-synuclein aggregates. Neuropathol. Off. J. Jpn. Soc. Neuropathol. 27, 494–506.

Wang, F., Nguyen, M., Qin, F.X.-F., and Tong, Q. (2007). SIRT2 deacetylates FOXO3a in response to oxidative stress and caloric restriction. Aging Cell *6*, 505–514.

Werner, H.B., Kuhlmann, K., Shen, S., Uecker, M., Schardt, A., Dimova, K., Orfaniotou, F., Dhaunchak, A., Brinkmann, B.G., Mobius, W., et al. (2007). Proteolipid Protein Is Required for Transport of Sirtuin 2 into CNS Myelin. J. Neurosci. *27*, 7717–7730.

Wu, Z., Puigserver, P., Andersson, U., Zhang, C., Adelmant, G., Mootha, V., Troy, A., Cinti, S., Lowell, B., Scarpulla, R.C., et al. (1999). Mechanisms controlling mitochondrial biogenesis and respiration through the thermogenic coactivator PGC-1. Cell *98*, 115–124.

Yang, X.-J., and Seto, E. (2008). Lysine Acetylation: Codified Crosstalk with Other Posttranslational Modifications. Mol. Cell *31*, 449–461.

Yiu, G., and He, Z. (2006). Glial inhibition of CNS axon regeneration. Nat. Rev. Neurosci. *7*, 617–627.

Yuan, Y.-H., Yan, W.-F., Sun, J.-D., Huang, J.-Y., Mu, Z., and Chen, N.-H. (2015). The molecular mechanism of rotenone-induced α-synuclein aggregation: emphasizing the role of the calcium/GSK3β pathway. Toxicol. Lett. *233*, 163–171.

Zhu, H., Zhao, L., Wang, E., Dimova, N., Liu, G., Feng, Y., and Cambi, F. (2012). The QKI-PLP pathway controls SIRT2 abundance in CNS myelin. Glia *60*, 69–82.

(2006). Neurological disorders: public health challenges (Geneva: World Health Organization).